

---

*Chapter 3*

**Compliant pneumatic muscle structures  
and systems for extra-vehicular and  
intra-vehicular activities in space  
environments**

*Samuel Wandai Khara<sup>1</sup>, Alaa Al-Ibadi<sup>2</sup>, Hassanin  
S. H. Al-Fahaam<sup>2</sup>, Haitham El-Hussieny<sup>1,3</sup>, Steve  
Davis<sup>1</sup>, Samia-Nefti Meziani<sup>1</sup>, and Olivier  
Patrouix<sup>4</sup>*

---

<sup>1</sup>Autonomous Systems and Robotics Research Centre, School of Science, Engineering & Environment, The University of Salford, Salford, M54WT, United Kingdom

<sup>2</sup>Computer Engineering Department, Engineering College, University of Basrah, Basrah, Iraq

<sup>3</sup>(on-leave) Electrical Engineering Department, Faculty of Engineering (Shoubra), Benha University, Cairo, Egypt

<sup>4</sup>ESTIA, 92 allée Théodore Monod, Technopole Izarbel, 64210 BIDART

In space environments, astronauts have duties that need to be addressed and some of them can be overwhelming, especially considering, in most cases, the crew members in the space station are normally a few. This can be resolved by accompanying the astronauts with assistant robots to reduce the workload. Thus,

deployment of soft robots, inspired by the morphological adaptation ability existing in octopus tentacles, elephant trunks, and snakes, is promising in a very long horizon for space exploration. In this chapter, we will discuss one of the soft robotic technologies we developed based on pneumatic muscle actuators' (PMAs) principle and show how they can be effective to improve the existing robotic systems that can be implemented in space environments. These developed PMAs are promising and can serve as alternatives to the traditional rigid robotic systems, by performing dexterous activities that are tedious, repetitive, and difficult to perform.

### **3.1 Introduction**

Recently, considerable literature has grown up around the theme of Human-Robot Collaboration (HRC) that is still in continuous development and improvement. Sectors like industry/manufacturing, households, and hospitals, even in extreme environments such as nuclear and subsea sites, are benefiting from the synergy in the collaboration between the human decision-making ability and the robot's accuracy [1]. Indeed, the form of such collaboration provided by robots to humans varies significantly according to the application or the mission that is required to be achieved. For instance, in harsh and unsafe environments, where it is risky for humans to have access, a teleoperated robot could be controlled remotely via a dedicated Human-Robot Interface (HRI) [2]. Moreover, robotics manipulators could also share the working environment and work closely and safely with humans in helping them achieving tedious, repetitive, and difficult tasks [3]. Rehabilitation and assistive robots are other forms of human-robot collaboration where either wearable or non-wearable robot systems aid human patients in enhancing their irregular body movements [4]. In space applications, robots such as Robonaut 2 (R2) [5] are playing a crucial role in HRC by relieving some repetitive and tiring duties from human space explorers due to their high dexterity and remote operation.

Inspired by the morphological adaptation ability existing in octopus tentacles, elephant trunks, and snakes, soft robots have proved the potential to facilitate the exploration of challenging environments [6]. Soft robotics is a novel approach in robotics that utilizes alternative flexible materials that are deformable to increase flexibility and controllability. It is a relatively new direction that has the potential to advance the robotics field as it has many benefits such as affordability due to its low cost, lightweight, safety, and morphological adaption ability. As

compared to rigid robots, soft robots have curvilinear structures with continually bending backbones that not only make them highly adaptable to the surroundings [6] but also allow sharing the working environment safely with humans [7]. Promising performance could be achieved by replacing rigid robots with soft continuum robots in fulfilling the desired tasks. However, several challenges need to be addressed. For instance, stiffness modulation is one of the crucial features that soft robots are better to have to be able to modulate their stiffness according to the required task at hand.

## 3.2 Robotic solutions for space environments

As early as 1991, one of the conferences held by NASA discussed Automation and Robotics for space-based systems, which discussed various proposals on how robotic systems such as manipulators could impact the space environments. Over time, it was considered that telerobotics and telepresence technologies could be utilized to reduce the crew extra-vehicular activity (EVA) and intra-vehicular activity (IVA) workloads in the international space station (ISS) [8]. The development of a ground teleoperated IVA robot was proposed to relieve astronauts from tedious and routine tasks, which could also provide ground researchers with a chance to interact and participate in space experiments.

A Dexterous Manipulator Development (DeManD) is an example of an EVA robotics for space station freedom suggested by Williams [9] to carry out specific tasks like inspection, workspace setup, and repair. Also, an IVA robotics for space station freedom was illustrated to demonstrate how it could increase productivity in conducting experiments using its automation technology. Besides, a Robotic Intravehicular Assistant (RIVA) was considered to be implemented inside a full-scale mock-up of a space station laboratory module to assist in protein crystal growth (PCG) experiments [10], demonstrating how robotic manipulators in space would be very essential in assisting astronauts even in their IVAs, where applicable.

On the other hand, humanoid robot such as R2 [11] has been developed to provide several benefits to the crew in the ISS by its advanced manipulators. It is an improvement of the Robonaut 1 (R1) developed by DARPA and NASA, which had the motivation of carrying out EVAs on behalf of astronauts [12]. The modifications on R2 were also meant to assist astronauts in maintenance tasks with minimal human supervision and R2 can reposition itself to different worksites, providing the ISS crew with more time to conduct other activities

[11]. The R2 is usually mounted on a rail to facilitate repositioning and aside from the hands, the legs as well have end effectors for holding tools to perform tasks independent of human input.

Although there is diversity of the mentioned robotics involvement in space applications, several directions are still promising and will show significant performance if robots have been incorporated. For example, traditional astronauts' spacesuit gloves are mainly designed for protection in harsh space environments while allowing astronauts to perform dexterous activities for EVA and IVA. However, existing gloves are made of many layers of insulating materials and tough fabrics to handle pressurization, warmth, and protection. For instance, the extra-vehicular passive spacesuit glove has reduced hand mobility by 10 percent due to its material that is designed to withstand pressure and thermal conditions [13]. One of the solutions to mitigate this issue, particularly in the gas-pressurized spacesuits and gloves, is to utilize the concept of mechanical counter pressure (MCP). So, spacesuits and elastic gloves are having counter pressures to meet the mobility challenges [14, 15]. The MCP concept is still undergoing research where the amount of counter- pressures needs to be in harmony with the hand movement, which mainly depends on the task. As an example, cable-driven power-assisted gloves were proposed in [16] to aid in improving the functionality of the pressurized spacesuit glove.

### *3.2.1 Soft robotic systems as an alternative robotic solution for space environments*

R2 and RIVA are rigid robotic structures that are susceptible to challenges when flexibility in confined and limited spaces and gentle interactions with humans are considered. As NASA's early implementation of one of the first IVA-type robotic manipulator systems in ISS, they highly stated that despite benefits acquired from the robot to assist in a specific task, the central area of concern is the crew's laboratory safety [17]. Soft robotic flexible structures can resolve some of these challenges since they pose less danger when interacting with humans and are relatively at a lower cost and much power efficient with a higher power to weight ratio.

Soft robotics is a relatively new field where soft materials and soft actuators are used to develop robot manipulators and grippers that are inherently safe to operate alongside people, possessing low mass and inertia, are often low cost, and have other abilities not offered by traditional rigid robots. Thus, we will

explore how dexterous soft robotic systems designed using PMA technology can offer a contributing solution to some of the mentioned challenges being addressed in space environments.

Space colonies will soon get to be established, and humans might start to settle in different places in space such as the Moon and Mars. In such environments, robots can play a crucial role, especially at the early stages when establishing the colonies in space, since the labor might be limited by the available human explorers at the site. Therefore, cost becomes a critical consideration for developing and manufacturing space robots. Both the academia and industries have been researching due to the several shortcomings faced by traditional robotic systems to develop different types of grippers, end effectors and manipulators to cut down the cost of the robotic systems and include additional abilities that allow handling and manipulation of a wide range of objects and materials [18]. Choi *et al.* [19] had a similar approach where the gripper can cost as much as 20 percent of the total cost of a whole robotic system. Meanwhile, the gripper design is limited to handling a specific object or a small range of objects. It could be expensive to manufacture grippers for varieties of objects each time and consequently could result in complex control systems. Hence, there is a need to develop systems that are low cost, multipurpose, with simple control burden wherever possible, and able to be integrated easily with existing robotics hardware. The development of new robotics designs, actuations, sensing, and control techniques is thus the different subfield contributing to the above discussions. Newer ways of designed actuators and their usefulness in space environments will be explained here.

One type of soft robots' actuation techniques is the PMA [20], which over recent years is shown to be a potential alternative to traditional actuators in existing manipulators and end effectors. PMAs have significant potential benefits due to their low cost, low weight, flexibility, and inherent softness [21].

Autonomous Systems and Robotics Research Centre at the University of Salford has been developing a soft robotic system using PMA technology. Some of the robotic systems include multi-fingered grippers designed based on novel Self-Bending Contraction Actuator (SBCA) and ring-shaped circular gripper that use the newly developed Circular PMA (CPMA). These new grippers are particularly well suited to grasping unknown objects as they naturally deform to the shape of the object being handled with their intrinsic flexibility. In the context of space applications, these soft robots are important for assisting inter-vehicular activities such as grasping of space rocks that might have irregular shapes and

textures and probably also are very delicate for handling. These gripper designs offer enhanced efficiency by eliminating the need for extensive grasp preplanning, having high payloads, minimal power requirements, and reduced control complexity. More of this based on their construction and experiments is explained later. Wearable soft robotics systems designed using the Extensor-Bending PMA (EBPMA) are also discussed and we will show how they can be beneficial for activities that require force augmentation to improve human performance when using the hands. A low-cost power assistive glove using the EBPMA is developed and experimented to demonstrate its ability to augment the user's strength and reduce fatigue. Such actuation technology for a glove can extend the abilities for a spacesuit glove worn by astronauts for either EVA or IVA.

### **3.3 Soft robotic systems based on PMA as an alternative to rigid robotic systems for space environments**

Soft robots are commonly made from soft and deformable materials and typically are not relying on traditional actuators. Instead, soft robots use soft actuation technologies and one popular actuator is the McKibben Muscle [22] known as the PMA. This actuator is formed from lightweight, soft materials, and being pneumatic it is compliant due to the compressibility of air. Thus, this mechanical property is the reason for replacing the rigid structures used in developing space robots, for example, manipulators and end effectors used to develop R2. In addition to the reduction of weight for safety most of such robots are still mounted on rails or supporting member structures. The weight reduction also improves power efficiency and ease of mobility.

The simplicity of McKibben muscle design is the reason for its popularity among PMA basic structures [22]. This PMA type is constructed by inserting a rubber tube inside a braided sleeve with caps at each end, one end is closed and the other left open, to let pressurized air in or out, see [Figure 3.1](#). For a contractor PMA at zero pressure, the tube and the sleeve have equal length and diameter, whereas for the extensor PMA, the sleeve is longer than the tube but of equal diameters. The braided sleeve angle governs the ability to change in length. If the braided angle is greater than 54.7 degrees (minimum energy state) the actuator will extend upon pressurization until reaching the minimum energy state.

And if the braid angle is less than 54.7 degrees, any pressurization allows the contraction of the actuator.

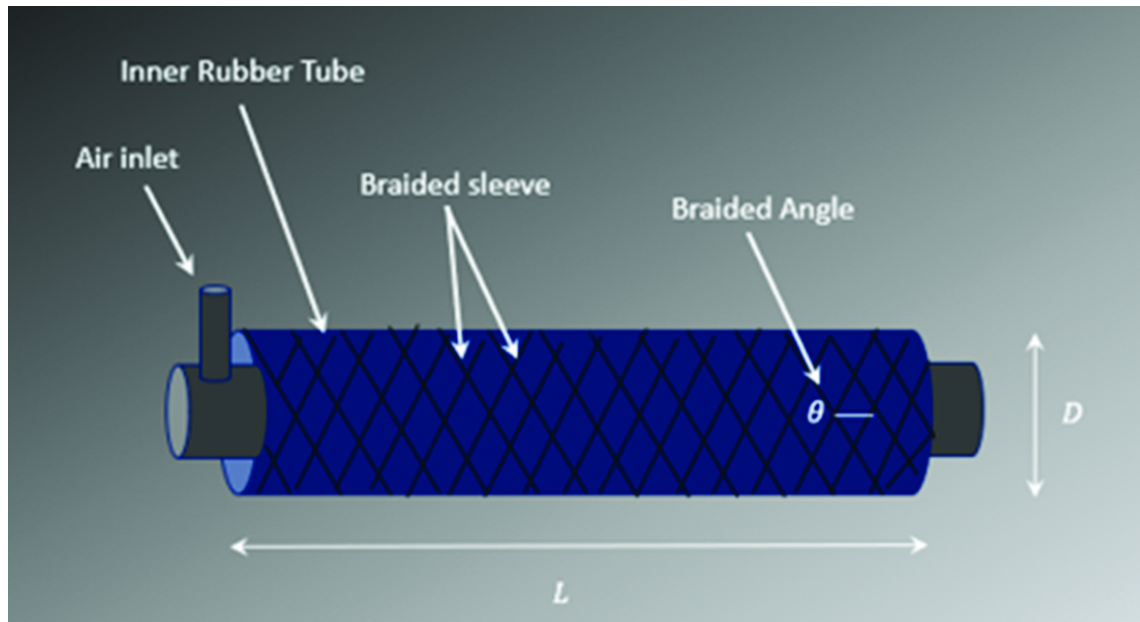


*Figure 3.1 The structure of the PMA, where  $L$  and  $D$  are the length and the diameter of the rubber muscle, respectively, at zero air pressure and  $\theta$  being the braided angle, which is the angle between the vertical line and the braided strand*

Behavioral analysis of the two types of PMA demonstrated their unique properties. A contractor and extensor PMAs of lengths 18.4 and 16 cm, respectively, and of diameters 5 mm were used in an experiment (Figure 3.2) to analyze changes in length upon changes in pressure between zero and 500 kPa at steps of 50 kPa (at no load). The contractor muscle reduced in length to 12.8 cm, about 30 percent reduction, and extensor increased to 25.1 cm, a 56 percent extension.

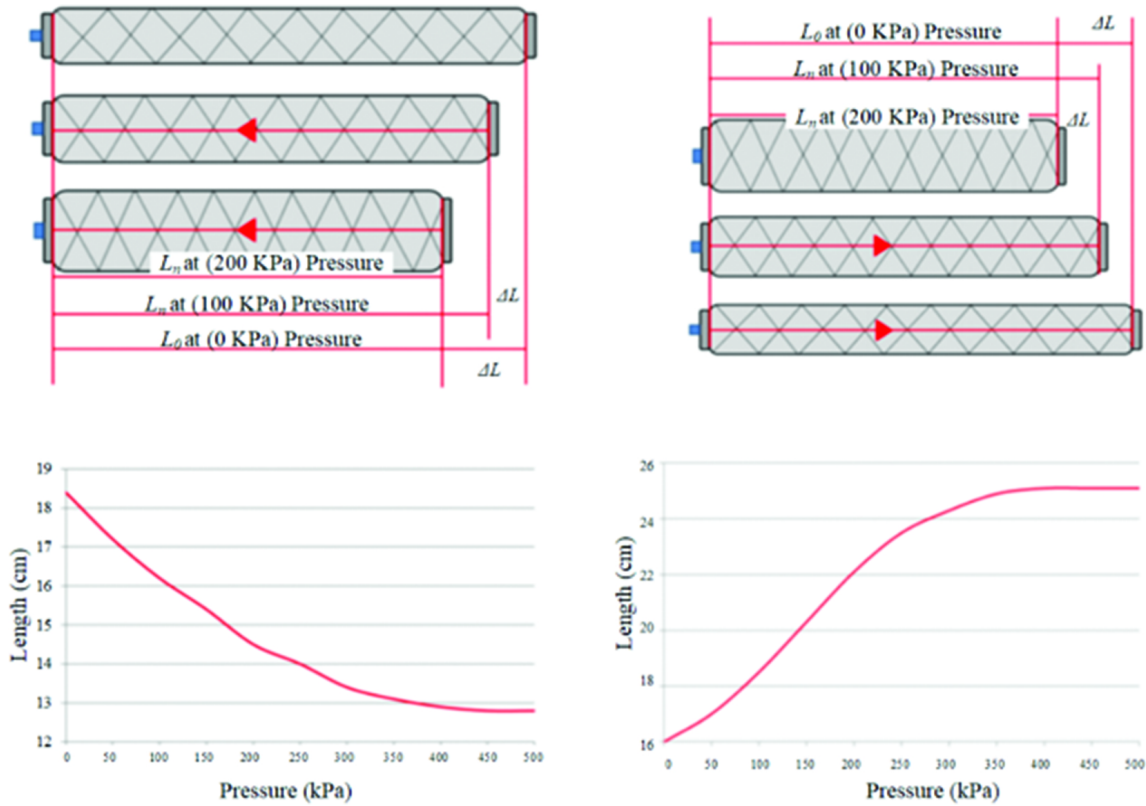


*Figure 3.2 Schematic representation of contractor and extensor PMA to the right and left, respectively, and their summary in length changes with respect to pressure changes*

The contractor PMAs possess similar behavior to the human muscles; they contract by thickening when pressurized. These are three distinguishable and crucial observations for the PMAs when in use [23, 24]:

- Isotonic characteristics: Varying input pressure under constant load, [Figure 3.2](#) on the left.
- Isobaric characteristics: Varying load under constant pressure input, [Figure 3.2](#) on the right.
- Isometric performances: Constant operation ratio by changing both pressure and load.

An experiment to investigate the three characteristics is done by fixing the contractor PMA at one end and mounting a load  $M$  on the other end ([Figure 3.2](#)) and applying incremental pressure from zero kPa to pressure  $P_1$  produces a pulling force equilibrium to the loading mass  $M$  [25]. As a result, the volume

increases to  $V_1$  and length reduces to  $L_1$ . Additional pressure to  $P_2$  further increases the volume to  $L_1$  and a length reduction to  $P_1$  until the maximum pressure is attained, which depends on the (sleeve and rubber) material properties of the PMA.

Figure 3.3 likewise shows the effects of variable load under constant pressure. Reduction of mass  $M_1$  to  $M_2$  decreases the length from  $L_1$  to  $P_1$ .

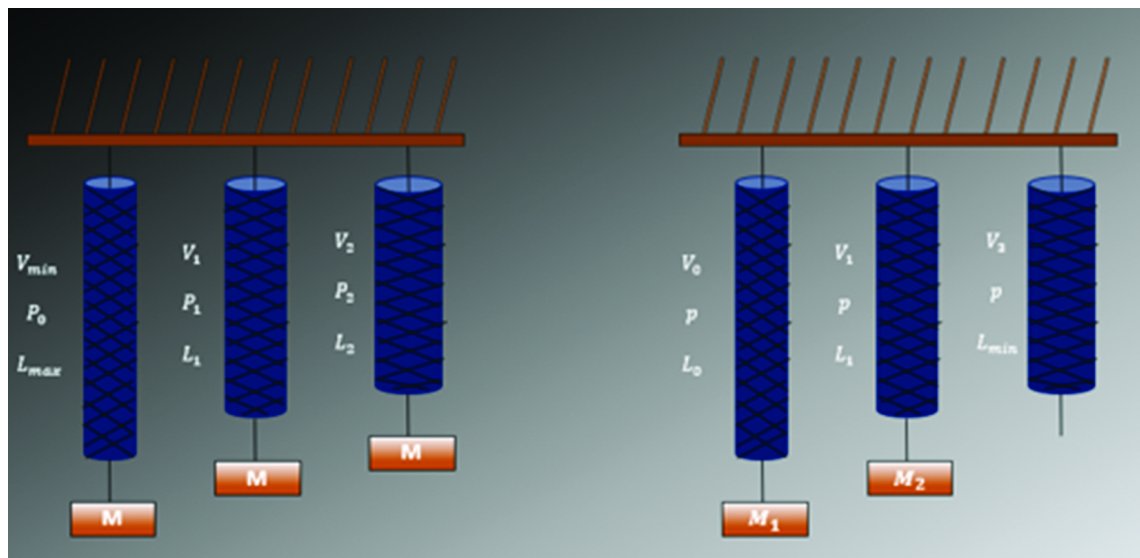


Figure 3.3 On the left the work of the PMA using constant load test and on the (right) is the constant pressure test of the PMA.

### 3.3.1 Modeling of a pneumatic muscle actuator

Most engineering systems must have quite accurate models that are useful in improving their behavior when implemented as part of a system [26]. Mathematical modeling of the PMAs is an ongoing process. One of the models relates the air pressure and the length of the PMA in generating a contractile force for the case of the contracting PMA. The model is affected by several factors, such as the properties of the materials used in the construction of the PMA, its length, its diameter, the braided angle, the air pressure, and the load force. Having a better understanding of their relationship enables the achievement of accurate models especially in developing a control model for the muscle [27].

One of the derived model [28] of a contraction PMA assumes that the PMA is cylindrical in shape, a contact point between the braided sleeve and the surface of the inner tube is always present, there is negligible friction between the rubber

and the braided sleeve and no considerations of the elastic forces in the inner rubber tube.

Using the parameters shown in [Figure 3.4](#) the work input  $W_{in}$ , for a McKibben's muscle under air pressure supply is given by (3.1):

$$dW_{in} = \int_{s_i} (P - P_0) dl_i \cdot ds_i = (P - P_0) \int_{s_i} dl_i \cdot ds_i = P_g dV \quad (3.1)$$

where  $\mu$  is the absolute pressure,  $P_2$  is the environment pressure ( $P_2 = 1.0336$  bar),  $\bar{m}$  is the gauge pressure (the relative pressure),  $s_i$  is the total inner surface,  $dl_i$  is the inner surface displacement, and  $dV$  is the volume change.

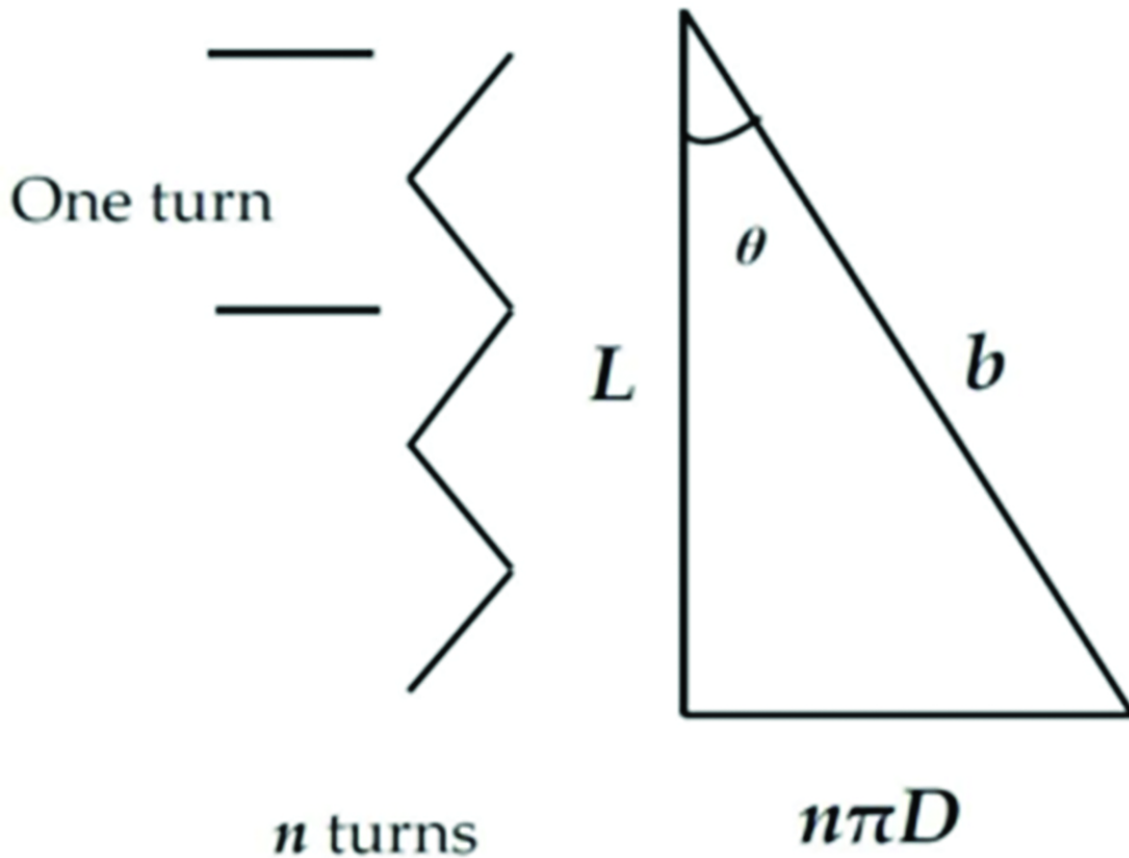


*Figure 3.4 The parameters of the PMA*

[Equation 3.2](#) shows the relation of how the change in work input  $W_{in}$  is proportional to the contractile force  $\Psi$  and change in axial length  $L$  of the

actuator.

$$dW_{in} = -FdL \quad (3.2)$$

Assuming the actuator has no storage of energy, then the input work will be equal to work output (3.3). The work output  $W_{out}$  is a result of the shortening of the actuator's length while dissipating a contractile force due to the change in volume and pressure input (3.4):

$$dW_{out} = dW_{in} \quad (3.3)$$

$$-FdL = P_g dV \quad (3.4)$$

$$F = -P_g \frac{dV}{dL} \quad (3.5)$$

$\frac{dV}{dL}$  assumes that the lengths of the strands of the braided sleeve are constant during the pressurization of the actuator. Thus, volume  $V$  of the muscle actuator is dependent on the length  $L$  and diameter  $D$ , which are given by (3.6) and (3.7).

$$L = b \cos \theta, \quad D = \frac{b \sin \theta}{n\pi}, \quad V = \frac{1}{4} \pi D^2 L \quad (3.6)$$

where  $b$  and  $n$  are constant, equation 3.6 assumes a volume of the actuator is in the form a cylinder:

$$V = \frac{b^3}{4\pi n^2} \sin^2 \theta \cos \theta \quad (3.7)$$

Hence the contractile force can be expressed as follows:

$$(3.8)$$

$$F = -P_g \frac{dV}{dL} = -P_g \frac{\frac{dV}{d\theta}}{\frac{dL}{d\theta}} = \frac{P_g b^2 (3 \cos^2 \theta - 1)}{4\pi n^2}$$

The mathematical model given by (3.8) illustrates that at maximum contraction when  $\Psi = 0$  the strands of the braided sleeve will be at  $\theta = 54.7$  degrees. This is one of the fundamental analyses demonstrating the basic behavior of this type of PMA. Further analysis is still on research by the robotics community to consider how friction, material deformation, elastic energy, and other factors affect energy losses in the system.

### 3.3.2 Characterization of contractor PMA

The characterization is a crucial step in developing an effective system. Therefore, using the force formulas for extensile and contractile muscles derived by [28, 29] gives useful insight into the performance of an actuator. However, it has been seen that despite the many models produced for pneumatic muscles they all contain errors that lead to inaccuracies. It is therefore prudent to experimentally investigate the behavior of the actuators before use. We did a study that involved a designed contractor and extensor PMA using different pressures and loading. The length of the contractor PMA was taken to be a function of air pressure and initial length. And further led to the modification of the contractile force formula [23, 29] to reduce the error between the experimental and model data. Additional study on the lengths and forces of both serial and parallel configurations of contractor PMAs was also done to observe the effects on different configurations and designs. Comparison analysis for a single extensor PMA and extensor PMA with multiple extensor PMAs connected in series was performed to determine their respective lengths and forces relationship on performance.

Figure 3.5 shows a contractor PMA with application of air pressure within the range of 0–500 kPa manually via a valve with increments of 50 kPa. The reverse process has also been done to reduce the pressure to zero and observe its hysteresis property. Table 3.1 is a summary of the different PMAs that were used in the experiment with varying lengths.



*Figure 3.5 Prototype of a contractor PMA used in the characterization experiments*

*Table 3.1 Specifications of a contractor PMAs under experiment*

<b>Nominal length <math>l_n</math> (cm)</b>	<b>Diameter <math>d</math> (cm)</b>	<b>Braided angle (<math>^\circ</math>)</b>
20	1.767	31.35
30	1.752	30.02
40	1.764	30.28

Figure 3.6 (a) shows a length change experiment for the contractor PMA's changes in length to changes in pressure. The recorded changes in length at a certain pressure level were determined by averaging the respective changes in length during the increase and decrease of air pressure. This was done to remove the hysteresis effect.

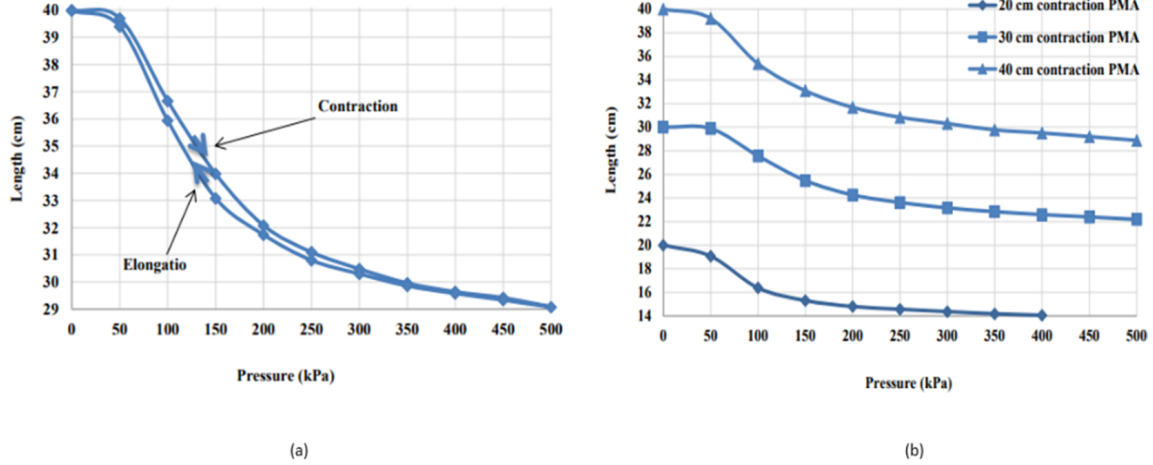


Figure 3.6 (a) Changes in length to changes in air pressure and (b) Experimental data for three PMA prototypes of different initial lengths of 20, 30, and 40 cm

$$\dot{L} = \frac{L_{n_{dec}} + L_{n_{inc}}}{2} \quad (3.9)$$

where  $0 \leq n \leq P_{max}$ ,  $L_{n_{dec}}$ , and  $L_{n_{inc}}$  are the contraction and elongation lengths, respectively. The  $\dot{L}$  is then used as the actuator length at respective points, Figure 3.6 (b).

### 3.3.3 Analysis of contractor PMA

The force modeling of contractor PMA conducted by Deimel *et al.* [29] served as the foundation of some underlying assumptions used for the modification of the model. The procedure involved experimental loading with varying weights: 0–10 kg in steps of 0.5 kg at the free end of PMAs that were of different lengths. The air pressure also was varied within a range of 0 kPa– $P_{max}$ , as summarized in Figures 3.7 and 3.8.

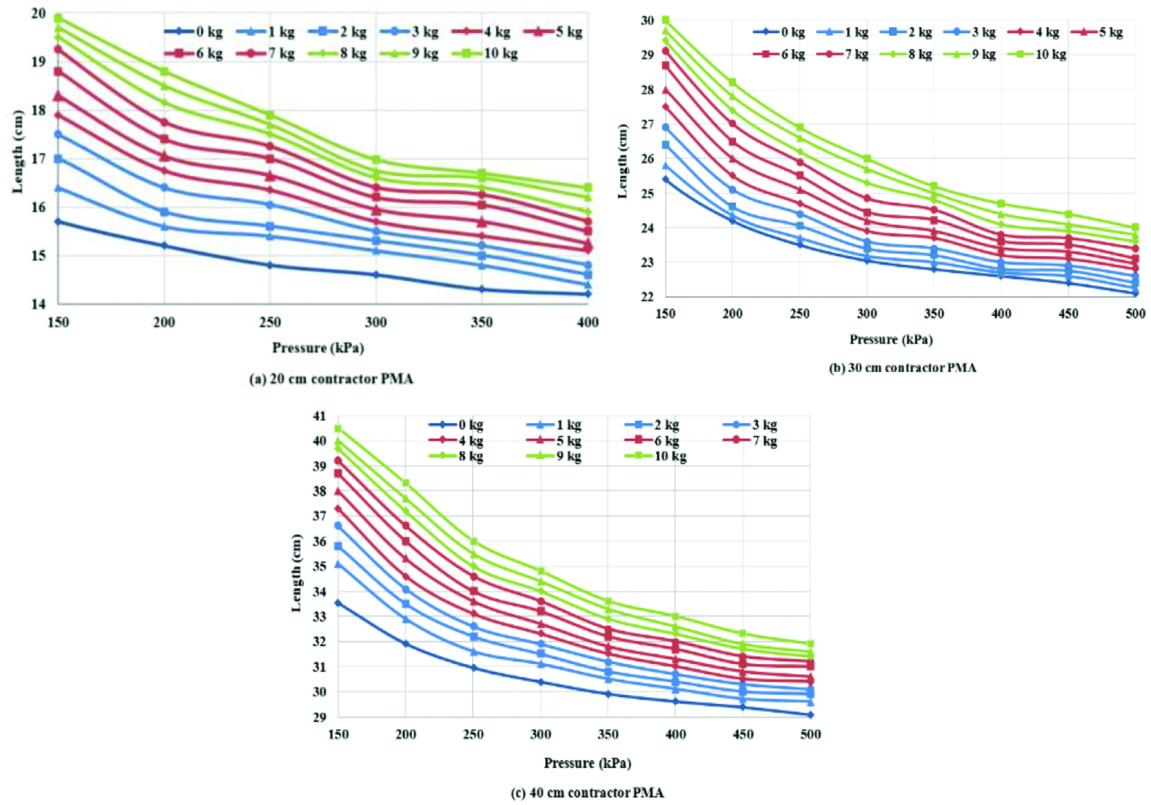
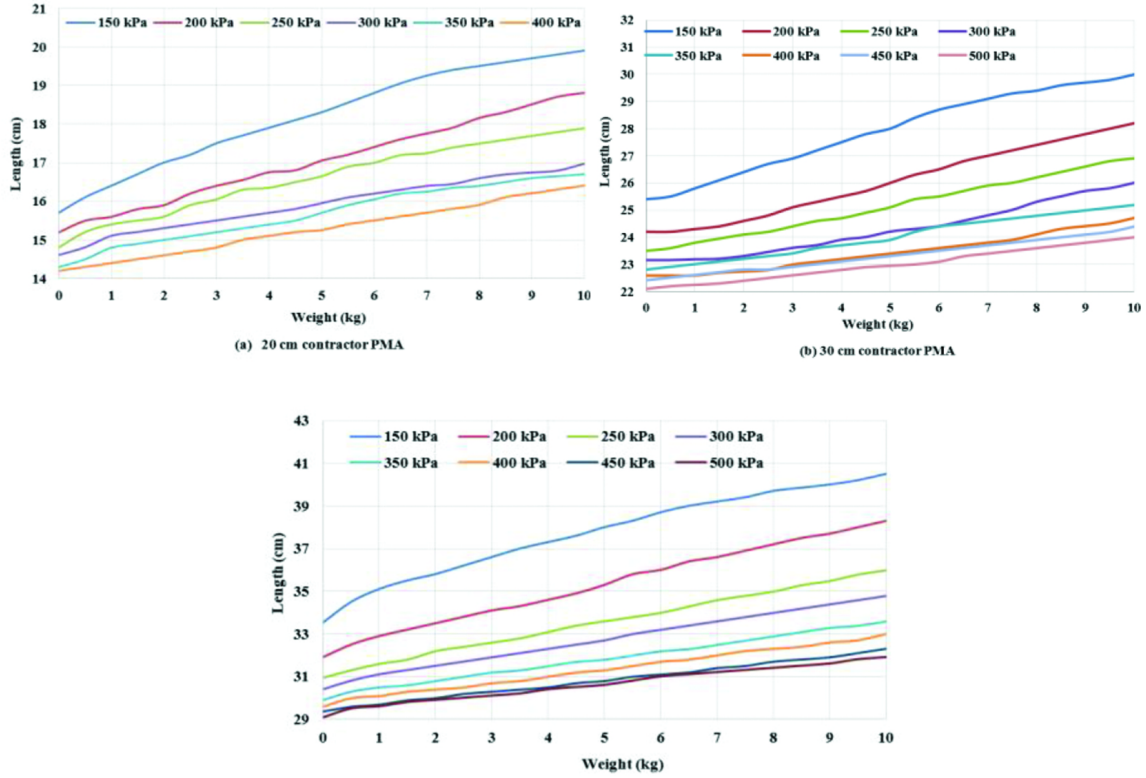


Figure 3.7 Changes in length of (a) 20 cm, (b) 30 cm, and (c) 40 cm PMA with respect to changes in pressure at fixed loadings



*Figure 3.8 Changes in length of (a) 20 cm, (b) 30 cm, (c) 40 cm PMA with respect to changes on loadings at fixed pressures*

In Figure 3.7, the contractor PMAs have similar behavior of change in length when loaded and pressurized at varying air pressure. They also showed a lower contraction ratio at higher loadings because of more downward force by the weight of the loads. The experiment recorded in Figure 3.8 showed an increase in length that is proportional to the loadings at fixed air pressure. At higher pressures, the increase in length is lower due to the generation of higher forces.

The model assumes the PMA is cylindrical in shape and there is constant contact between the inner rubber tube with the outer braided sleeve [22]. However, in practice, this is not the case and the factors vary with actuator design. A correction factor  $\tau$  is therefore introduced but highly dependent on the PMA structure. In a test actuator, full contact of the rubber and sleeve occurs only above certain pressure  $\mu$ ; in the experiment, it was found to be 45 kPa for the PMA prototype. The resulting modified force  $f$  is seen in (3.10):

$$(3.10)$$

$$f = \pi r_{0centers}^2 (P - 45) \left[ \alpha (1 - q\varepsilon)^2 - \beta \right], \quad P \geq 45 \text{ kPa}$$

where  $\alpha = \frac{3}{\tan^2 \theta}$ ,  $\varepsilon = \frac{L}{L_0}$ ,  $\beta = \frac{1}{\sin^2 \theta}$ ,  $q = 1 + 1e^{-0.5P}$  while  $\theta$  is the braided angle, and  $r_{0centers}$  is the radius of the outer braided sleeve.

Figure 3.9 (a) and (b) are plots of force against pressure for practical experiment and theoretical data using (3.11) and (3.10), respectively. The difference with the two line graphs is because of the underlying assumptions of cylindrical in shape and continuous contact of the sleeve and the rubber tube. Additionally, Figure 3.9 (b) shows how the modified formula did manage to map the theoretical plot to closely resemble the experimental plot.

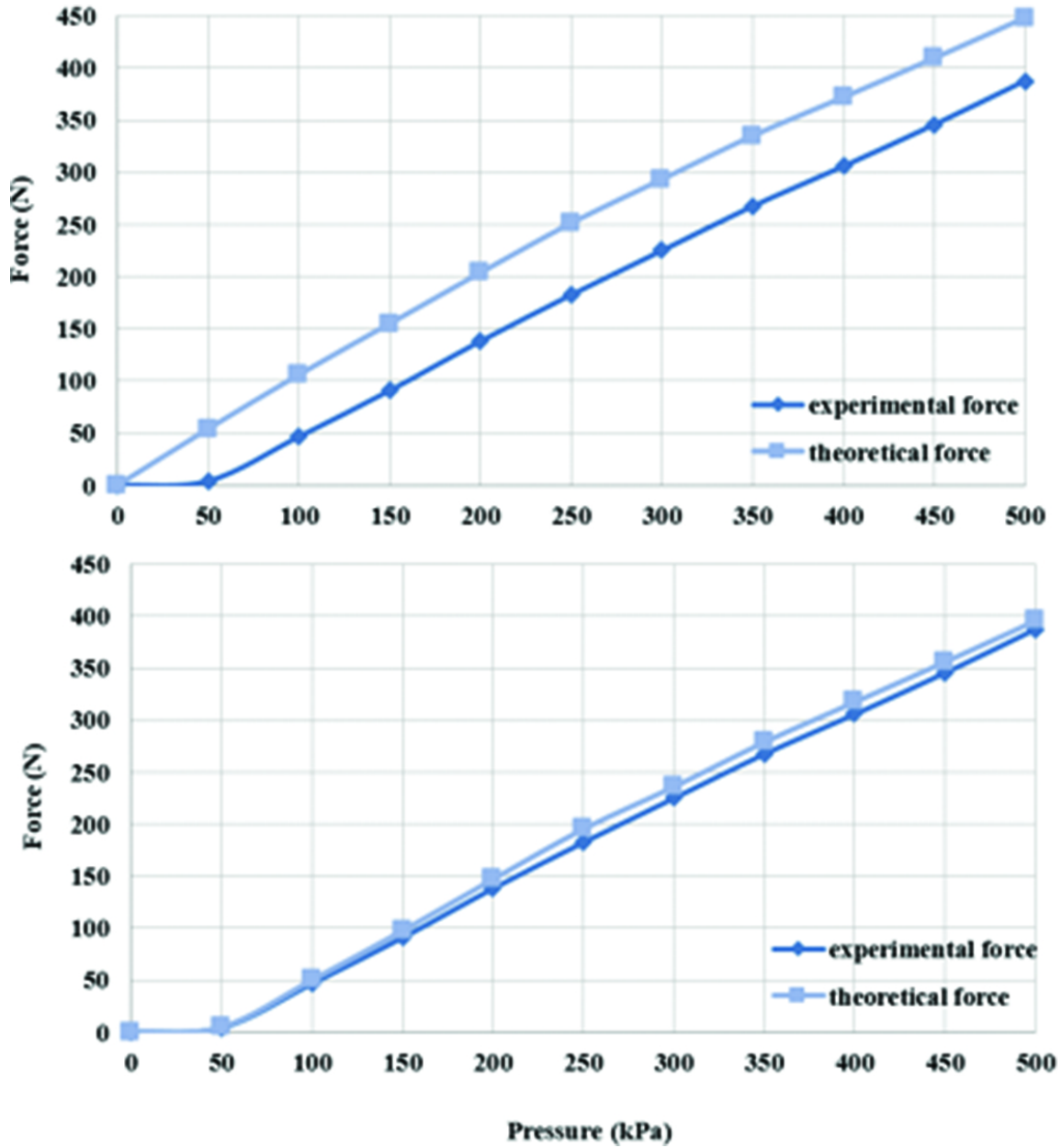
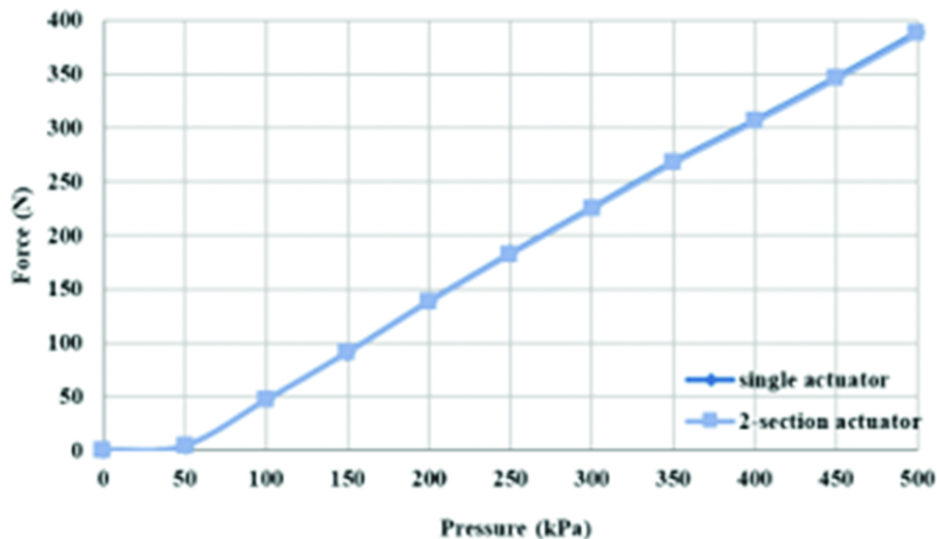


Figure 3.9 Experimental and theoretical force analysis for a 30 cm PMA using (3.10) and (3.11)

$$f = \pi r_0^2 (p) \left[ \alpha (1 - q\varepsilon)^2 - \beta \right] \quad (3.11)$$

A comparison performance experiment for multiple actuators arranged in series versus a single PMA was conducted. This involved prototypes of two 30 cm

contractor PMAs in series and a single contractor PMA of 60 cm in length. The plot in Figure 3.10 shows that the force generated by the two actuators in series is like that of a single actuator of the same length. However, the serial arrangement provides a degree of redundancy, should one of the actuators faults the other will continue to operate.



*Figure 3.10 Two 30 cm PMAs connected in series and its comparison force results to a single 60 cm PMA, showing their similar output results by having their line graph overlapping each other*

Multiple actuators could also be arranged in parallel to each other. A continuum arm was constructed by arranging several PMAs in parallel. Figure 3.11 depicts a 30 cm contractor PMA arm with four actuators; one at the center and the other three are positioned 30 mm away from the arm's center to their axial centers and are separated  $120^\circ$  apart from the neighboring actuator.



Figure 3.11 Prototype and mechanical design of the fixed and free end of the four parallel actuators for the continuum arm [30]

A comparison experiment of a single contractor PMA and the continuum PMA arm with four parallel actuators was performed as recorded in Figure 3.12 (a). Both actuator systems did contract by the same amount when pressurized since each actuator was of similar in design. The slight variations between the results are caused by friction between the four actuators. When analyzing the force output, the force generated by the parallel actuators is approximately four times that of a single PMA when each of the four actuators is pressurized at equal pressures, Figure 3.12 (b). The relation of force  $\Psi$  produced by multiple actuators can be generalized by (3.12).

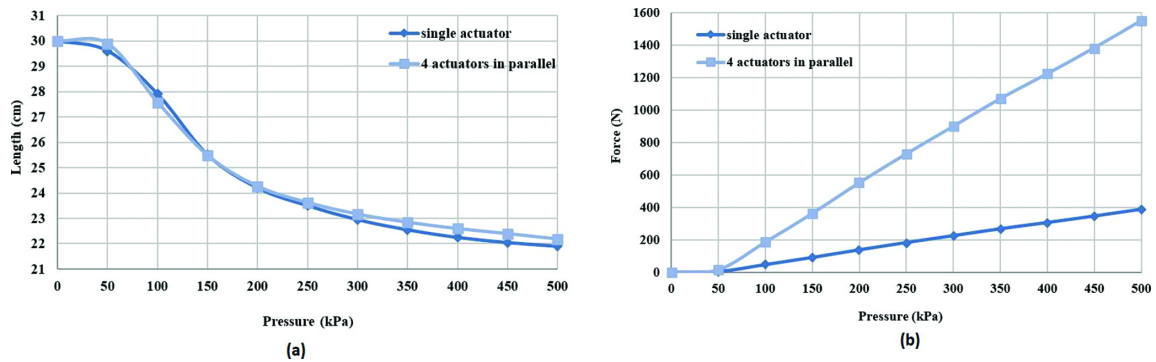


Figure 3.12 Comparison experiment for a single contractor PMA and a continuum PMA arm with four parallel actuators, (a) length-pressure characteristic and (b) force-pressure characteristic

$$F = Kf \quad (3.12)$$

where  $K$  is the number of parallel muscles and  $f$  is the force of a single muscle.

The above experiments were based on pressurizing the four actuators with the same value and this results in a linear contraction of the continuum arm. However, if each of the muscles was supplied with different pressures, each would contract by differing amounts causing the actuator to bend and thus behaving like a continuum arm. This is demonstrated by supplying a fixed pressure to two of the outer actuators, while the remaining actuator is supplied with increasing pressure from 0 to 500 kPa. The bending angle  $\theta$  of the four actuated arms is shown in Figure 3.13 (a) and it can be seen that the bend angle is dependent on the amount of pressure. The maximum angle  $\theta$  is affected by the amount of loading as observed from the line curves in Figure 3.13 (b), with the heavy loadings resulting in a smaller maximum angle.

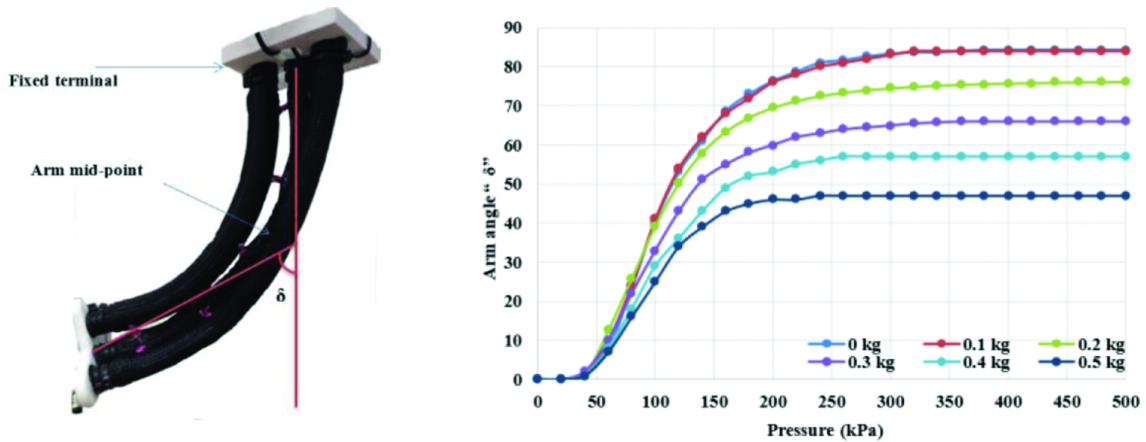


Figure 3.13 On the left, a contractor PMA continuum-arm with bending angle, and on the right a bending angles relative to loading values

### 3.3.4 Modeling of extensor PMA

Experiments for an extensor PMA are similar to the contractor PMA. Figure 3.14 shows changes in length, which increases with an increase in air pressure to a maximum length determined by a fixed length of the braided sleeve.

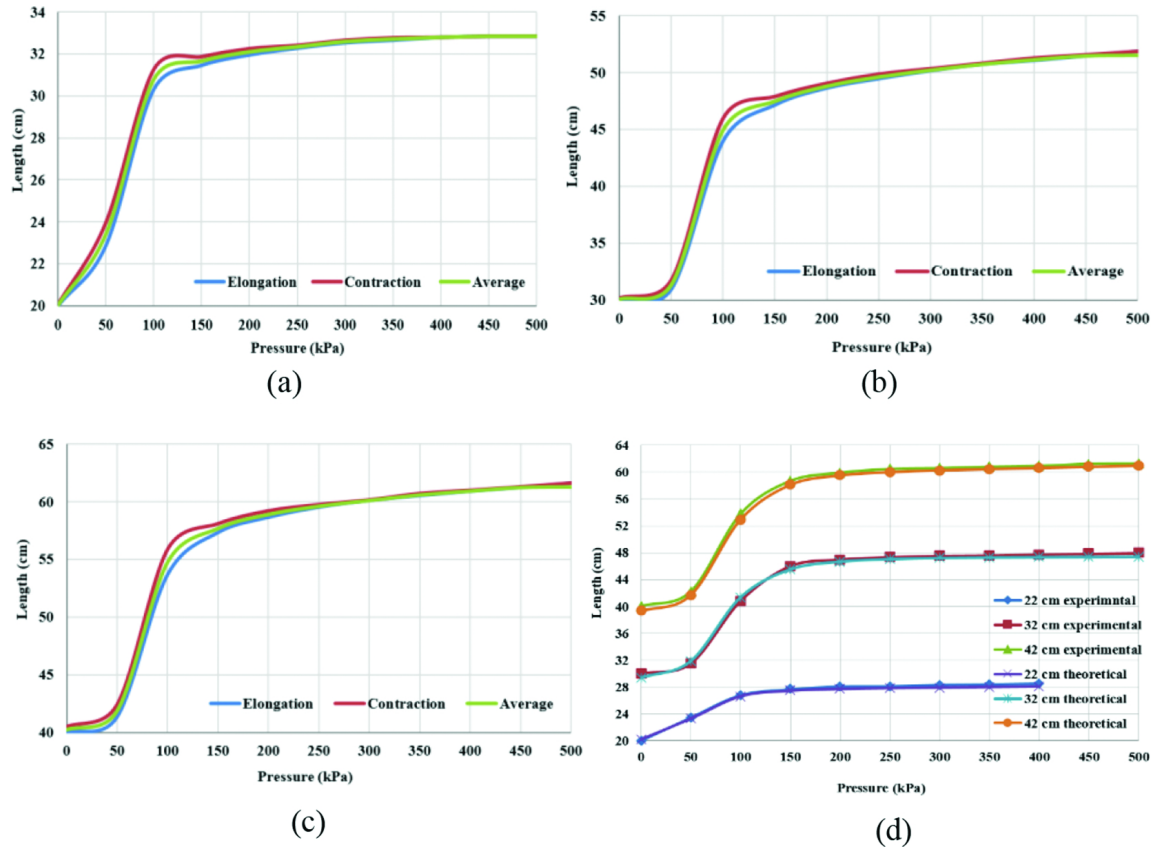
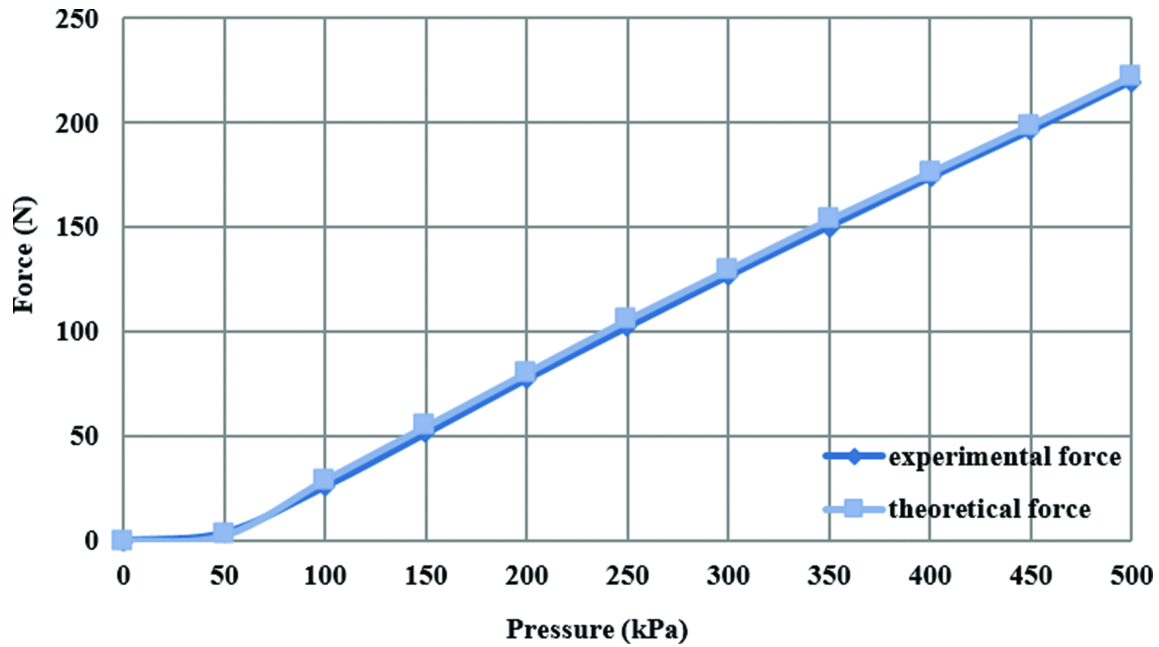


Figure 3.14 Change of actuator length against air pressure for (a) 20 cm, (b) 30 cm, (c) 49 cm PMA, and (d) practical and theoretical lengths against pressure changes

The modified force formula for an extensor PMA also includes the initial 45 kPa pressure as its zero-force value (3.13), which shows the change in direction of force with a minus sign. Figure 3.15 gives the relationship of the force generated and the pressure input for experimental and theoretical values, the variation is a result of the contact between the rubber tube and the braided sleeve.

$$f = -\pi r_0^2 (p - 45) [\alpha (1 - q\varepsilon)^2 - \beta], \quad p \geq 45 \text{ kPa} \quad (3.13)$$



*Figure 3.15 Practical and the presented theoretical force for a 30 cm extensor PMA*

Experimental analysis recorded in [Figure 3.16](#) shows changes in length due to pressure changes for the extensor PMA under fixed loadings while [Figure 3.17](#) has the pressure values fixed with varied loadings. The observations show that the elongation due to loadings is much less at higher pressures.

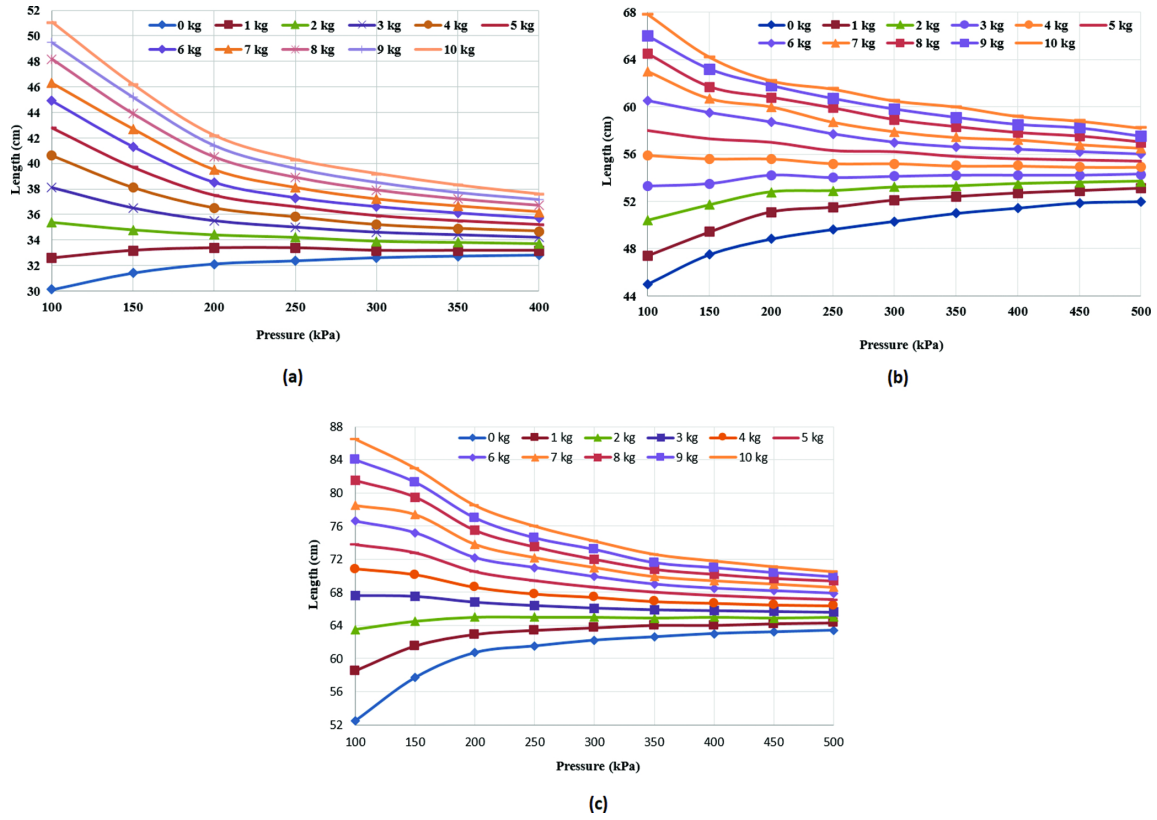
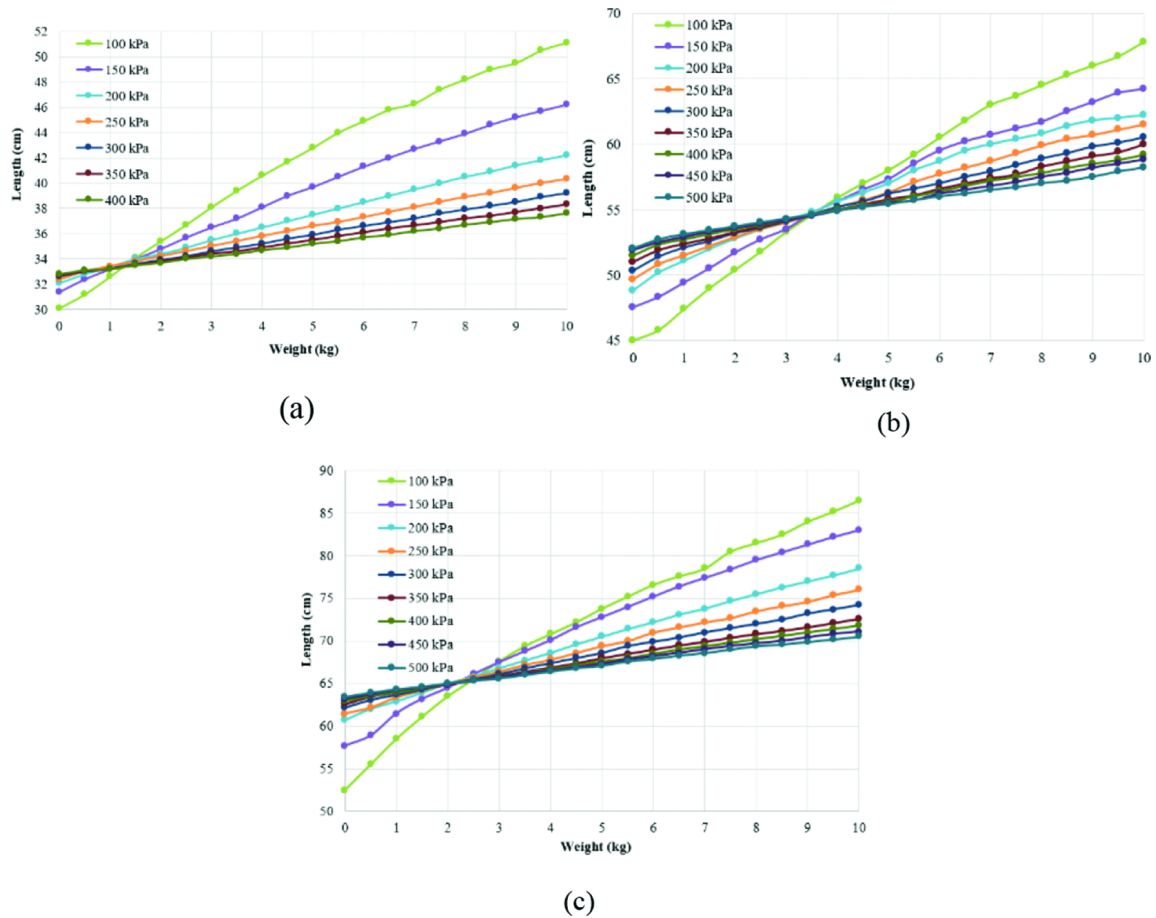


Figure 3.16 Changes in length of (a) 20 cm, (b) 30 cm, and (c) 40 cm PMAs at varying loads with fixed pressures



*Figure 3.17 Changes in length of (a) 20 cm, (b) 30 cm, and (c) 40 cm PMAs at varying loads with fixed pressures*

An extensor PMA continuum arm with four actuators that can bend in all directions is designed as shown in [Figure 3.18](#) (b) (whose fundamental working principle is discussed in the [Section 3.4](#)). Each of the four actuators is of length 30 cm, [Figure 3.18](#) (a), one at the center and the other three are 3 cm away from the center of the arm and are  $120^\circ$  apart from the neighboring actuator.

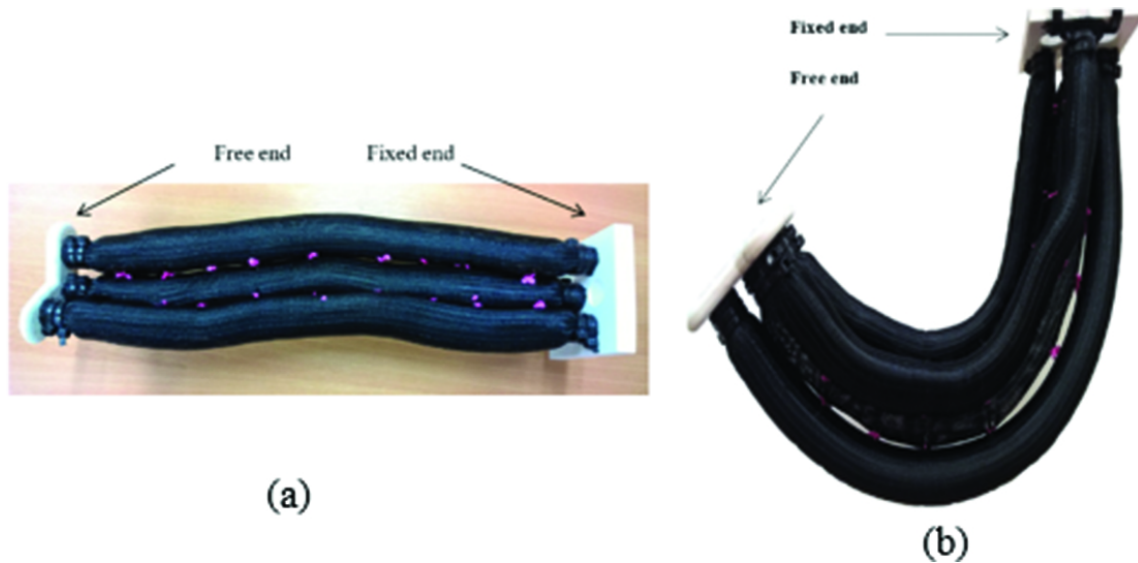


Figure 3.18 (a) A four extensor PMA continuum-arm (b) at a certain bending angle when pressurized [30]

When the air pressure is equally distributed to the four PMAs, the continuum arm extends but bends towards the direction of PMA with the highest distribution. The bending angle is dependent on the amount of weight attached at the free end. Figure 3.19 (a) shows the most acute angle is attained at lower loadings.

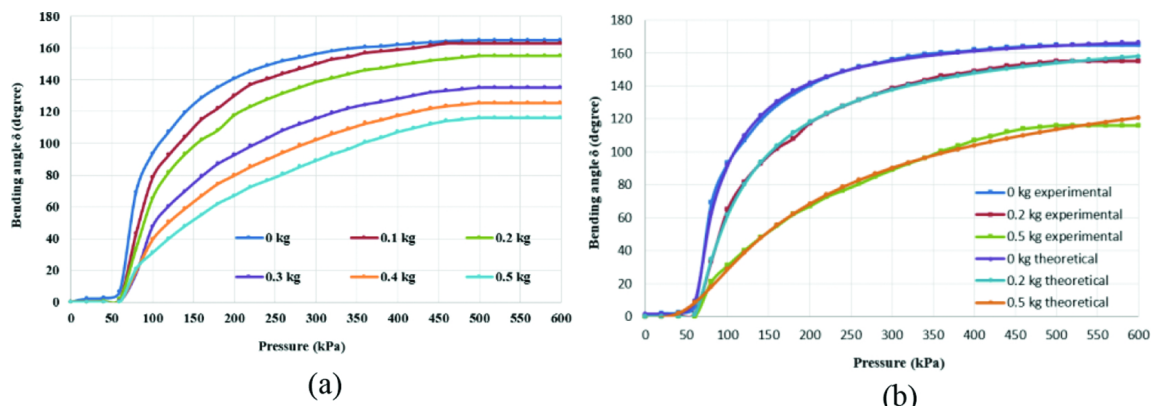


Figure 3.19 Result analysis for the four extensor PMA continuum-arm. (a) The bending angle against the pressure at different load conditions and (b) comparison of experimental and theoretical bending angles at three different load conditions.

## 3.4 PMA designs that can be adapted as robotic manipulators for space

The work in this section involves design concepts using the techniques discussed in [Section 3.4](#). These unique designs have promising results of how they can be an alternative to the rigid manipulators, since they are extremely flexible and possess infinite degrees of freedom, making them ideal to do tasks that are challenging to achieve with rigid manipulators. Their simplicity in construction and lesser weight are good achievements when accounting for transporting robotic system to space and when mounting them on rails in the space station. These systems have not tested yet in low-gravity settings to emulate space environments and are currently under investigation as part of the FAIR-SPACE project.

Both the contractor and extensor PMAs discussed in [Section 3.3](#) generate linear motion or force that acts in one direction. However, some modification produces novel actuator designs that can produce bending motions, some that can contract or extend in length, a ring design for gripping action. This section gives the detailed explanations of self-bending PMAs, double-bending PMA, extending and contracting PMA, and CPMA.

### *3.4.1 Self-bending contraction actuator and extensor-bending pneumatic artificial muscles*

Bending motion of the PMAs can be achieved by preventing one side of the actuator from changing length when the opposite side extends or contracts. Two types of bending muscles include an EBPMA and the SBCA.

The EBPMA is created by longitudinal fixing along one side of an extensor PMA as depicted in [Figure 3.20](#). This fixing takes the form of an inextensible thread that prevents one side of the muscle from extending when pressurized. This is the same principle used in the construction of the extensor PMA continuum-arm with four parallel PMAs discussed earlier. If the actuator is pressurized, the free side of the muscle extends and because the thread on the opposite side limits changes in length, a bending motion occurs as depicted in [Figure 3.20](#).



*Figure 3.20 An EBPMA at bending when pressurized at 300 kPa  
[30]*

The SBCA is a biologically inspired design that imitates how bones support surrounding muscles. The bending actuator prototype is formed from a contraction PMA that has a thin flexible rod of 2 mm width inserted in between the rubber tube and braided sleeve, as seen in [Figure 3.21 \(a\)](#). The rod prevents one side of the actuator from contracting when pressurized while the other side contracts freely, [Figure 3.21 \(b\)](#). Just like the EBPMA, this mismatch between displacements causes a bending motion. Comparing the payload capacity made by these two bending designs is an ongoing experiment at the time of writing this chapter.

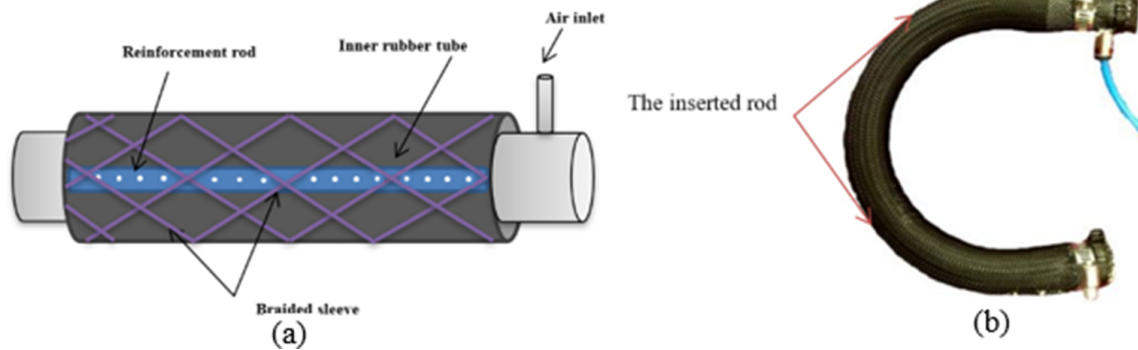


*Figure 3.21 (a) SBCA with a flexible rod inserted between the braided sleeve and rubber tube and (b) 30 cm SBCA pressurized at 300 kPa [31]*

### *3.4.2 Double-bending pneumatic muscle actuator*

The bending muscle presented above are only capable of bending in a single direction; however, by reinforcing different sections of the muscle it is possible to create more complex bending motions, for example, the prototype shown here can bend in two directions. It is based on the SBCA by placing two flexible rods on opposite sides of the PMA, a distance apart on either half of the length, resulting in a bending behavior shown in Figure 3.22 (c), which forms an S shape when pressurized.

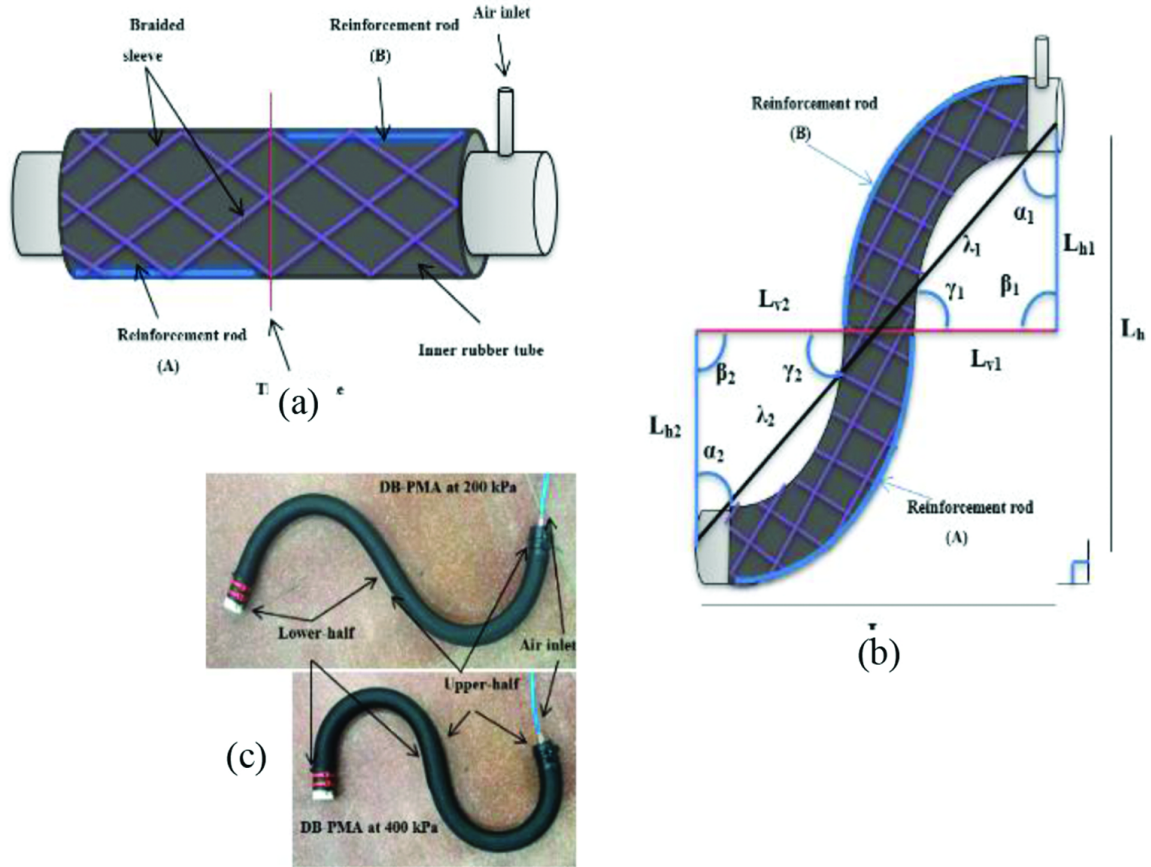


Figure 3.22 (a) The structure of the double-bend pneumatic muscle actuator (DB-PMA), (b) the bending behavior and the geometrical analysis of the DB-PMA, and (c) DB-PMA at different pressure values of 200 and 400 kPa

Identical reinforcement rods of similar material and size result in a symmetrical shape for the upper and lower half of the actuator, Figure 3.22 (b). Despite the simplicity of the design and minimal usage of resources, the actuator can move in both the horizontal and vertical directions using one actuator. The calculation of the vertical or horizontal length,  $P_1$  and  $P_2$ , of the actuator is given by (3.14).

$$L_v = (\lambda_1^2 + L_{h1}^2 - 2\lambda_1 L_{h1} \cos\alpha_1) \frac{1}{2} + (\lambda_2^2 + L_{h2}^2 - 2\lambda_2 L_{h2} \cos\alpha_2) \frac{1}{2} \quad (3.14)$$

$$L_h = (\lambda_1^2 + L_{v1}^2 - 2\lambda_1 L_{v1} \cos\gamma_1) \frac{1}{2} + (\lambda_2^2 + L_{v2}^2 - 2\lambda_2 L_{v2} \cos\gamma_2) \frac{1}{2}$$

where  $\lambda_1$  and  $d_{r1}$  are the two rods diagonals while  $\alpha_1$ ,  $\alpha_2$ ,  $\gamma_1$ , and  $\Psi$  are the angles defined in [Figure 3.22](#) (b).

This design means that by appropriately positioning the reinforcement rods, a complex bending motion can be achieved. As such it could be used to develop soft fingers capable of forming a bending shape desirable to certain grasping actions, for example, two metal rods, each one is at the formed trough.

### 3.4.3 *Extensor-contraction pneumatic muscle actuator*

The two types of PMA discussed earlier can independently provide either pulling or pushing forces. However, each type is only capable of producing either of the forces but not both. This means that they must be used in pairs or to work together with another mechanism such as a spring to provide reversed motion. Unfortunately, in applications where space is limited, it might be desirable to combine the two PMAs into one single device that can provide the two forces in a more compact and convenient package. Hence, an extensor-contractor PMA (ECPMA) has been developed by inserting a contractor muscle inside an extensor muscle. All pneumatic muscles contain a “dead space” inside them since the force produced by the muscle is not based on the inside volume of the actuator but the surface area of the inner tube. This means this inner volume can be exploited by inserting another PMA without affecting the actual forces the outer PMA can provide.

The ECPMA has modified end caps to host the contractor element inside the extensor muscle: two inlets to supply air in each of the respective muscle types as shown in [Figure 3.23](#) (a). From the ECPMA’s resting length, if the extensor PMA is pressurized the actuator will extend to its maximum length limited by the outer sleeve. When the contraction PMA is pressurized, it contracts past the extensor PMA resting length until reaching maximum reduction in length. Therefore, depending upon the relative pressures within the extensor and contraction PMA, the actuator can lengthen or shorten and produce tensile or compressive forces.

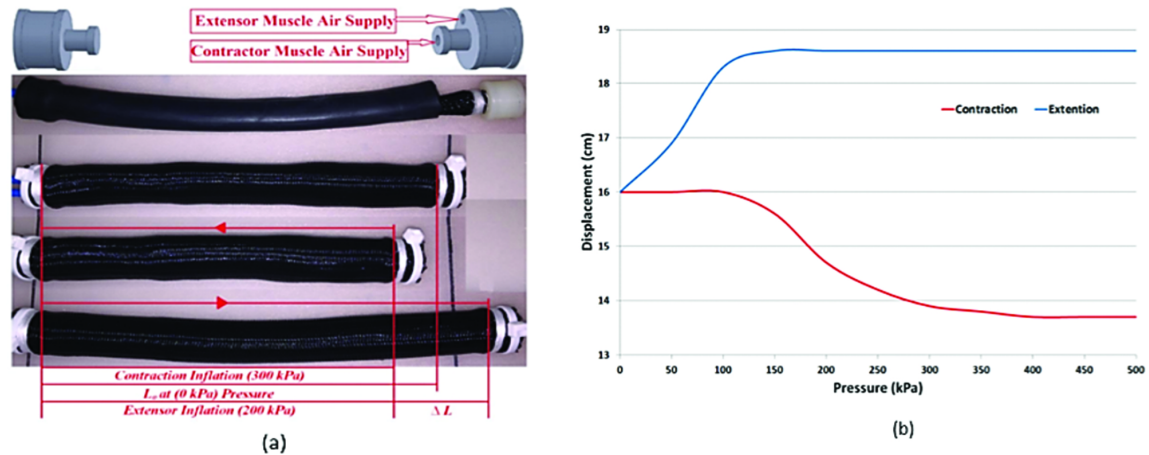


*Figure 3.23 (a) The modified caps with two inlets for air supply and three state of the ECPMA depending on pressure input (initial length, contraction, extension). (b) Change in length of ECPMA when pressurizing the two muscles independently*

Figure 3.23 (b) shows the experimental results obtained for the new actuator. It has a resting length of 16 cm and when the extensor PMA is pressurized, it extends to 18.6 cm. When the contraction PMA is pressurized, the actuator shortens to approximately 13.7 cm. Therefore, unlike a conventional PMA, this variation can both extend and contract depending on relative pressure in the two PMAs.

Figure 3.24 shows how the force measurements in the ECPMA was experimentally conducted. The actuator was mounted between a fixed surface and load cell and it was pressurized to predefined testing pressures, and the respective forces on the load cell were measured and recorded. The pressure in the contraction PMA was then increased incrementally, which reduced the actuator length, and the pulling force was measured by the load cell when the pulling force created by the contraction PMA exceeded the pushing force by the extensor. The load cell also measured the generated pushing force, which increased in proportion to the increase in pressure input. Thus, the actuator can produce both a pushing force and a pulling force on the load cell. The transition point between these two is dependent on the relative pressures in the types of PMA.

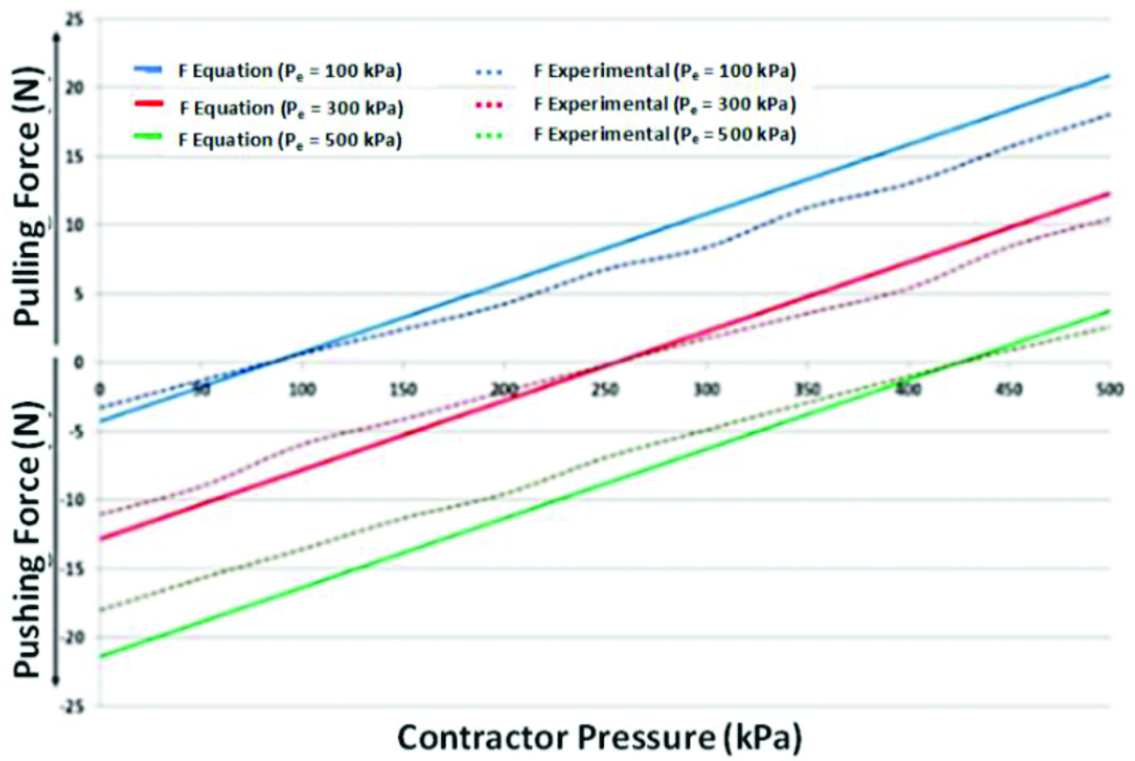
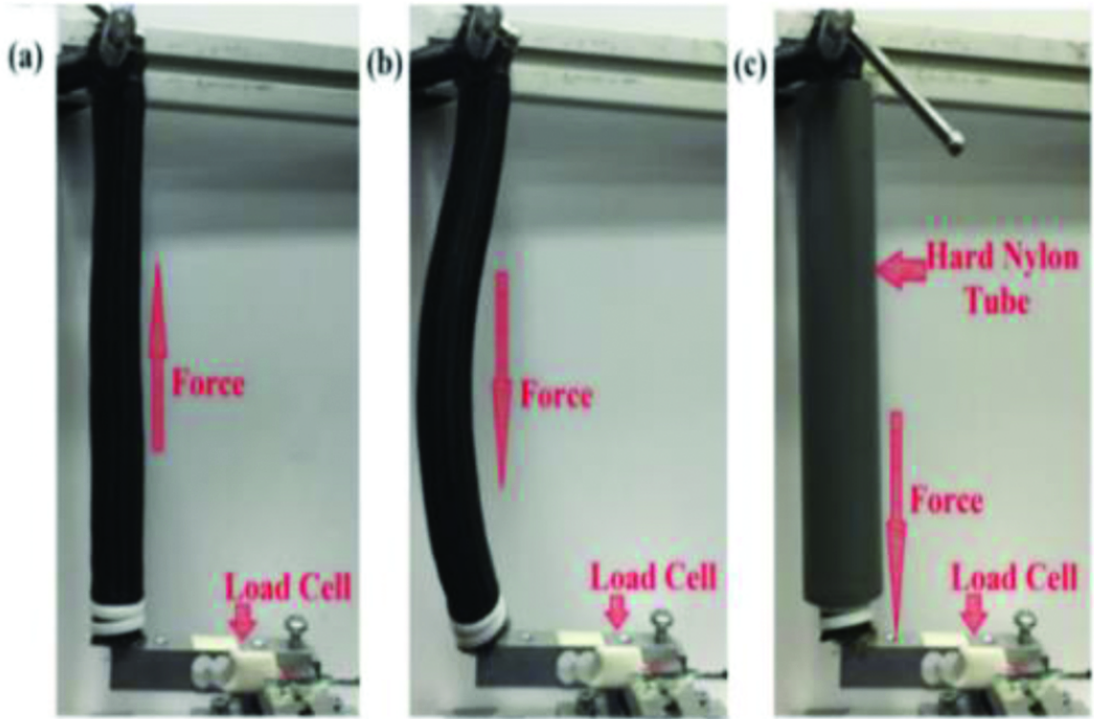


Figure 3.24 Dimensions of the CPMA on the left and on the right, the actual experiments for its validation

### 3.4.4 Circular pneumatic muscle actuator

Another interesting PMA design concept is the CPMA, which is inspired by facial muscles around eyes and mouth. It is designed to shrink its inner circumference and increase the diameter of the actuator. This is achieved by joining the ends of a contraction PMA to form a ring as seen in Figure 3.25. Increasing the air pressure reduces the circumference of the actuator, which in turn reduces the inner and outer diameter of the CPMA.

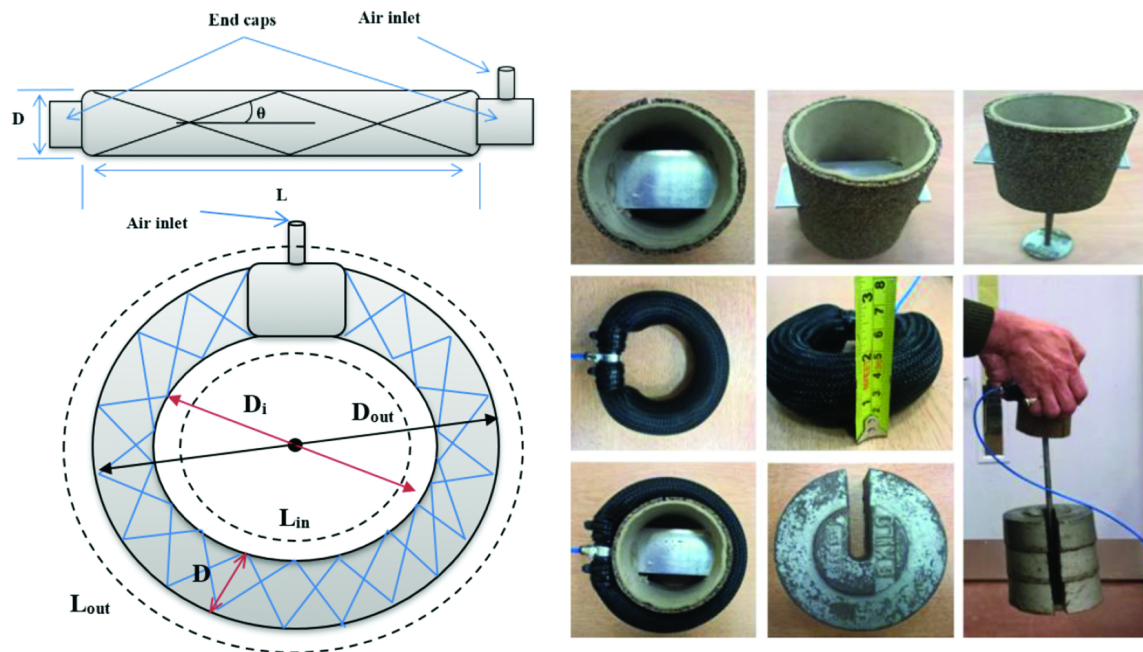


Figure 3.25 Dimensions of CPMA and actual experiments for its validation [32]

The reduction of the inner diameter generates a radial force towards the center of the ring, which in turn is applied to any object placed within it. In Figure 3.25 the CPMA is being used to grasp a circular object. When pressurized, the actuator tightens around the object and the resultant force in conjunction with friction between the actuator and object helps for a secure grasp.

## 3.5 PMA applications in developing novel grippers, manipulators, and power assistive glove for space

## environments

In this section, some design concepts of soft robotic grippers and manipulators are explored using the above pneumatic muscle actuation technologies. These grippers have been designed with improvements in mind of the limitations offered by some of the already existing technologies in providing similar services. As pointed out earlier, weights of components making up a robotic system can become a challenge by itself, especially if efficiency in power consumption or motion control is to be considered. Irregular objects are also a challenge when being handled by the end effectors of robots. And in some cases, the rigid end effectors are not suitable to handle delicate objects, especially the handling of space rocks during experiments is critical. Thus, the following alternative soft grippers and manipulators are designed to be compliant and light in weight, of which they can be adapted for improving the existing robotics systems in IVAs in the space station or future space colonies. The power assistive glove discussed will be demonstrating how the technology can be useful for augmenting force to human fingers, to aid in better grasping and handling of objects. This particularly aims at the spacesuit glove used by astronauts since the pressurization and stuffing of many layers affects the mobility of the fingers. Therefore, in addition to the limitation by design, the astronaut's hands also get the natural muscle fatigue especially amplified by countering the spring back effects of the inner pressure contained by the glove, which in turn causes a reduction in performance. In the future, the power assistive space suit gloves could then be able to assist astronauts while performing their IVA and EVAs.

The [Section 3.4](#) has presented a range of designs derived from the conventional operation of PMAs, and they have been used to develop a three- and six-fingered gripper, extension-circular gripper, and varied manipulators.

### *3.5.1 Three fingers gripper base on SBCA*

The SBCA described in [Section 3.3.1](#) can be used to construct a multi-finger gripper to aid in compliant grasping. A prototype soft gripper is constructed using three identical 14 cm long SBCAs that act as the fingers. The actuator only flexes when pressurized. Thus, an elastomeric material is placed on the rear of each finger to spread out the actuators when deflated. The fingers can spread 20 cm apart and touch each other on closure when pressurized, which makes them suitable to grasp a wide range of object sizes.

A rigid and noncompliant gripper requires some elements of grasp planning and precision control for each finger when handling certain objects. However, this design relieves such requirements as its ability to automatically bend around and deform to suit the shape of the objects irrespective of the complexity in shape. This ability means there is no need for grasp preplanning or sophisticated control; the gripper can operate well even with open-loop control. When activated, the finger bends and makes contact with the target object and continues to wrap itself around it. Each finger in the prototype has a maximum bending angle of 72 degrees, which allows them to touch each other at the center of the gripper. This property allows the soft gripper to handle small-sized objects of less than 10 mm (e.g. a pen) or much larger complex-shaped parts.

A further modification to the design included the addition of three shorter fingers as seen in Figure 3.26. This has the benefit of being able to grasp objects more securely and increases the grasping force as well. Experimental results that used a prototype soft gripper weighing 0.34 kg could achieve a maximum payload of 3.6 kg.

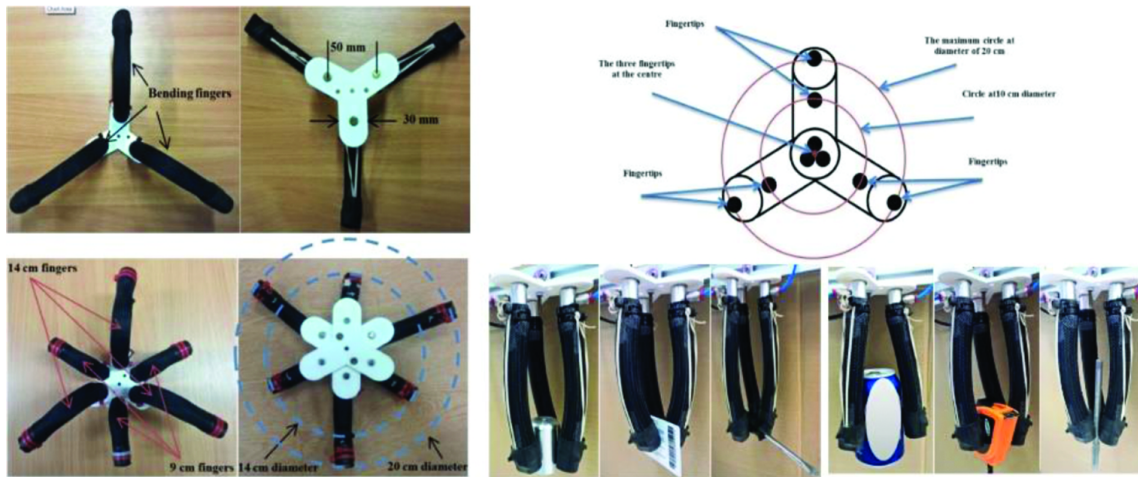


*Figure 3.26 A three and six-fingers gripper based on SBCA handling different objects and a diagram representation of the three-finger design's fingertip at different positions within its workspace*

The potential applications of this gripper in space environments can be very useful in the handling of unknown and undefined objects like space rocks, which may vary in physical properties: weight, shape, and fragility. This is something

that traditional grippers struggle with: demanding extensive preplanning, which is difficult to achieve without a geometric model of the object to be grasped or extensive sensor, especially visual data. Thus, the grasping of objects can be slow and inefficient. Therefore, the potential applications of this gripper design can be for extra-vehicular to capture space debris. By its very nature, this debris is often of unknown shape and size and this gripper would be able to grasp the debris with relative ease as the fingers deform and conform to the object being grasped automatically and rapidly without the need for extra operations or extensive planning. Similarly, the gripper could also be suited to the collection of samples on other terrestrial bodies, which again will likely have unknown geometry, and especially when teleoperation can be limited due to communication latencies.

### *3.5.2 Extension-circular gripper*

A very different soft gripper has been created using the CPMA highlighted in [Figure 3.27](#). Unlike many common soft grippers, this design does not have flexible fingers, instead it operates by deforming the shape of the gripper around the object to be grasped. The prototype soft gripper is constructed from three 18 cm extensor PMA and one 30 cm long CPMA with a maximum diameter of 7.8 cm. The extensor PMA provides the ability to direct and extend the gripper to the target object to be grasped while the CPMA does the actual grasping action by contracting around the target object and applying a compressive force to its entire periphery.



*Figure 3.27 The structure of the extension-circular gripper also showing its ability to grasp objects of different shapes and center axis [32]*

The extensor muscles allow the gripper to extend from 18 cm in length to 24 cm. Therefore, to grasp an object the gripper is placed above the target and then the extension muscles are activated to extend the gripper. This pushes the circular gripping element towards the target object. The benefit of this design is that the soft nature of the gripper means that should the target object has an odd pose, the natural compliance of the extensor muscles will cause the gripper to flex to automatically align the circular element with the target object appropriately. This is usually a challenging task for rigid grippers since they lack bending ability. Once located as desired, the CPMA is pressurized and reduces to a minimum diameter of 4.45 cm, which is a 43 percent reduction. This applies compressing force to the outer edges of the target object leading to a firm grasp.

This extension-circular gripper has an advantage over a multi-finger in that it has infinite contact points with the target object while a gripper with fingers is limited to the number of available fingers being used to grasp. The size of the object that the gripper can handle is determined by the maximum and minimum

diameter of the CPMA, which for the case of our prototype means target object must be between 4.45 and 7.8 cm across. However, the design is fully scalable, and larger and smaller designs can be created to match a range of target objects.

### 3.5.3 Three CPMAs gripper

The previous gripper design consists of a single CPMA that limits the grasp force of the gripper, especially if the object to be grasped is long and large, meaning that the grasp is only applied over a relatively small part of the target object's length. The extension-circular gripper has been modified by increasing the number of CPMAs to three, raising the grasping payload and increasing the gripping surface area. In this prototype [Figure 3.28](#), the extensor muscle can vary from 27 to 38.1 cm, which is a 41 percent extension, whereas the CPMA grasping diameter ranges from 8 to 4.3 cm at 0 to 400 kPa, respectively, which is a 46 percent reduction in diameter. The weight of the gripper is 0.8 kg and it could lift a 6 cm wide cylinder of 40 kg as demonstrated in [Figure 3.28](#).

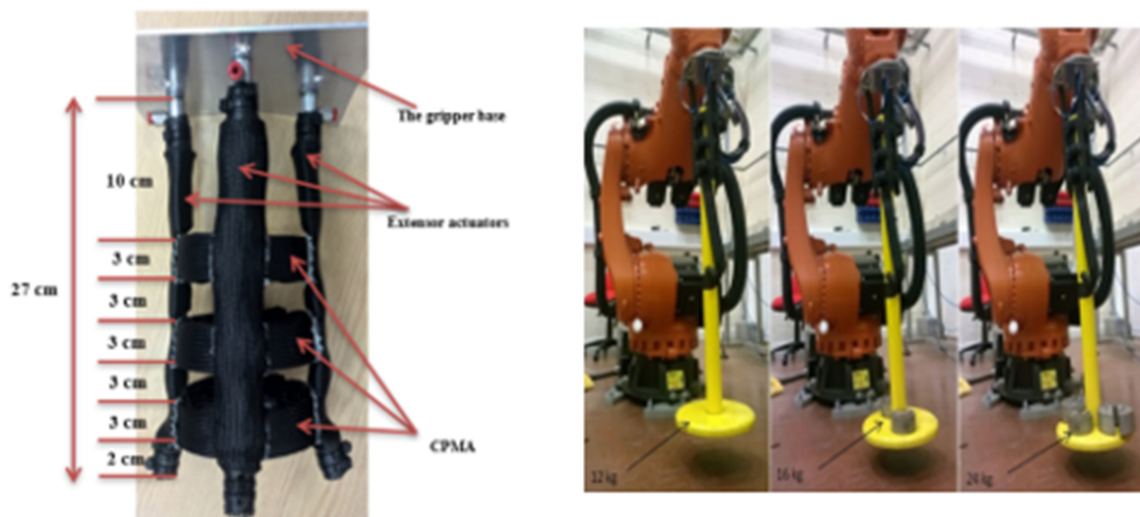


*Figure 3.28 The dimensions and the structure of the three CPMA gripper and a grasp lifting experiment at different loadings [30]*

Just like the soft gripper consisting of fingers, the main application for this type of gripper in space environments would be best suited where the geometry of the target objects is unknown. These could be samples of space rocks collected or parts of debris needing retrieval. The main advantage of the gripper is the fact that grasp force is spread over a large area instead of specific

localized points and this makes it particularly well suited to handling delicate and easily damaged samples.

### 3.5.4 *Soft robot manipulators*

In addition to producing the soft grippers using PMA designs, the concept can be extended to create soft robotics manipulators. In [Figure 3.29](#) we see contraction and extensor PMA are combined to form two continuum manipulators. As was described in [Section 3.2](#), a continuum manipulator can be formed by arranging multiple muscles in parallel. Depending upon the relative pressures in each of the muscles, the manipulator will flex and bend. The manipulators do not have individual discrete joints but instead, the entire body of the system flexes. [Figure 3.29](#) also shows a single-section and a two-section manipulator. The multi-section version has a greater workspace as each section moves independently of the other. Both systems have a high power-to-weight ratio, each weighing less than 1 kg but can carry payloads of up to 7 kg.

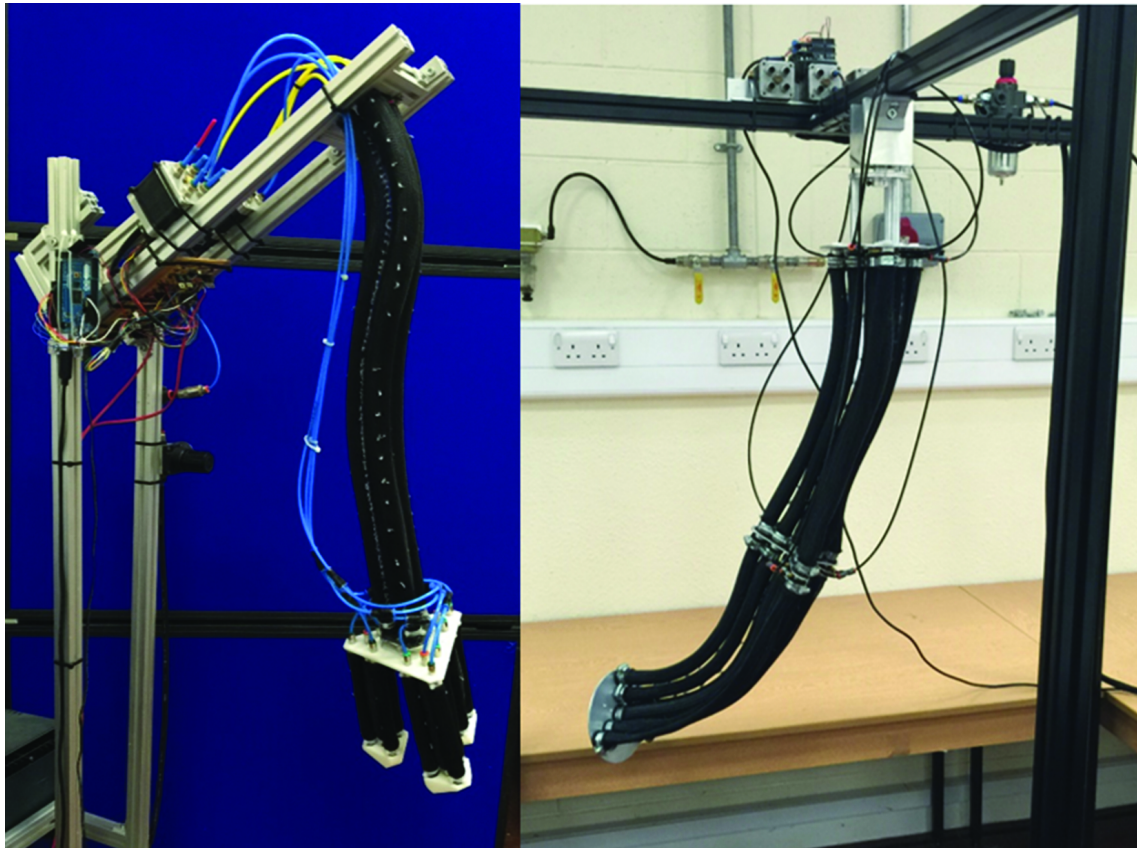


*Figure 3.29 Two manipulator designs that can flex in all direction of a workspace to handle objects using their attached grippers at the free end [31]*

An alternative design of continuum manipulator can be created using the SBCA described previously, see [Figure 3.30](#). Here the direction of bending is not a function of the differential pressure in the muscles but is determined by the construction of the self-bending actuators. This means the system has a more limited workspace, but it is mechanically simpler, has lower cost and is much less complex for a control model. This design is well suited where a specific motion must be of high repeatability, for example, a pick and place type motion. Though with appropriate design modifications for the system, complex behaviors can still be achieved, as seen in [Figure 3.30](#), where two manipulators are working together to relocate a sample cylindrical object.

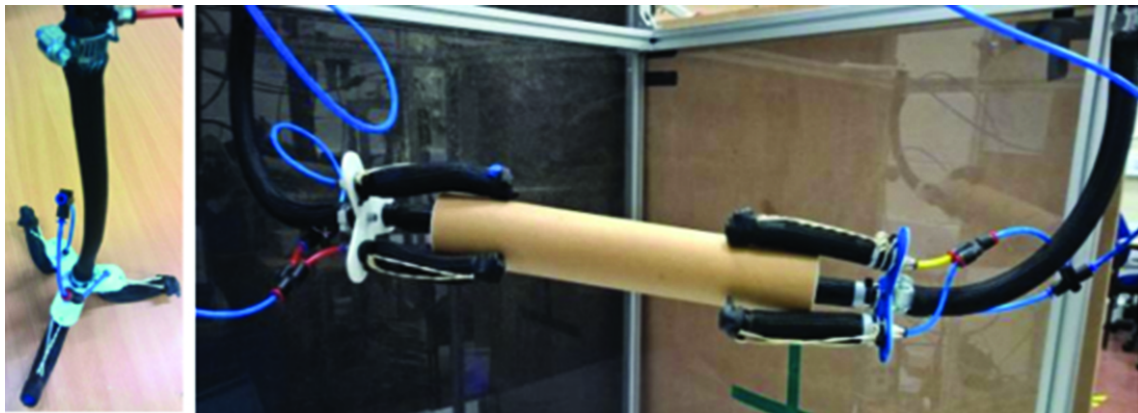


*Figure 3.30 A single bending continuum arm and the three fingers gripper with two of them performing a collaborative task*

Soft manipulators have several potential applications in space environments. Their lightweight makes them less costly to get to orbit as payload weight has a significant effect on launch cost. The systems are also potentially at a lower cost to manufacture than the traditional robots due to the materials used. However, such systems are still a long way from being produced commercially. In the future, this could reduce the cost of building and deploying remote robotic systems.

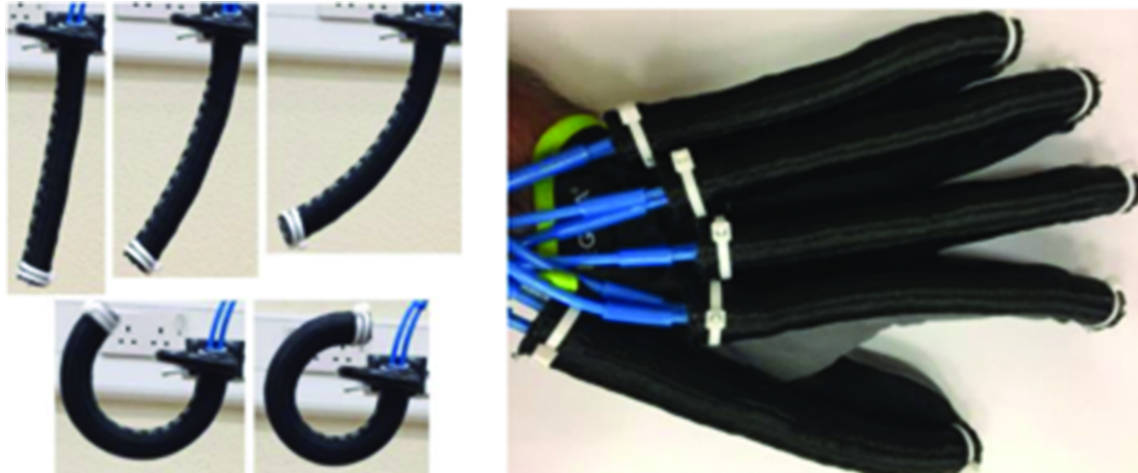
Soft arms also have the potential to offer safer alternatives to conventional robot arm in terms of both the safety of astronauts and other mission hardware. The soft arms are lightweight, have low inertia, and are compliant, which mean should they collide with an astronaut there is fewer chances of an injury. Also, because they deform on contact with objects the contact forces become spread over a greater area, meaning less likelihood of causing damages to other objects when a collision occurs.

Soft robot manipulator could work safely alongside astronauts to aid in completing tasks through collaborative working. Soft manipulators could even be mounted to an astronaut's suit to operate as an additional limb and enhance their productivity during EVAs. One of the other benefits is that as the soft continuum arms do not have discrete joints and can deform around obstacles, they can access locations where traditional manipulators struggle, like a constrained path to an object. This enhances the range of tasks that robots could be used to perform in an uncertain space environment.

### *3.5.5 Power assistive soft glove*

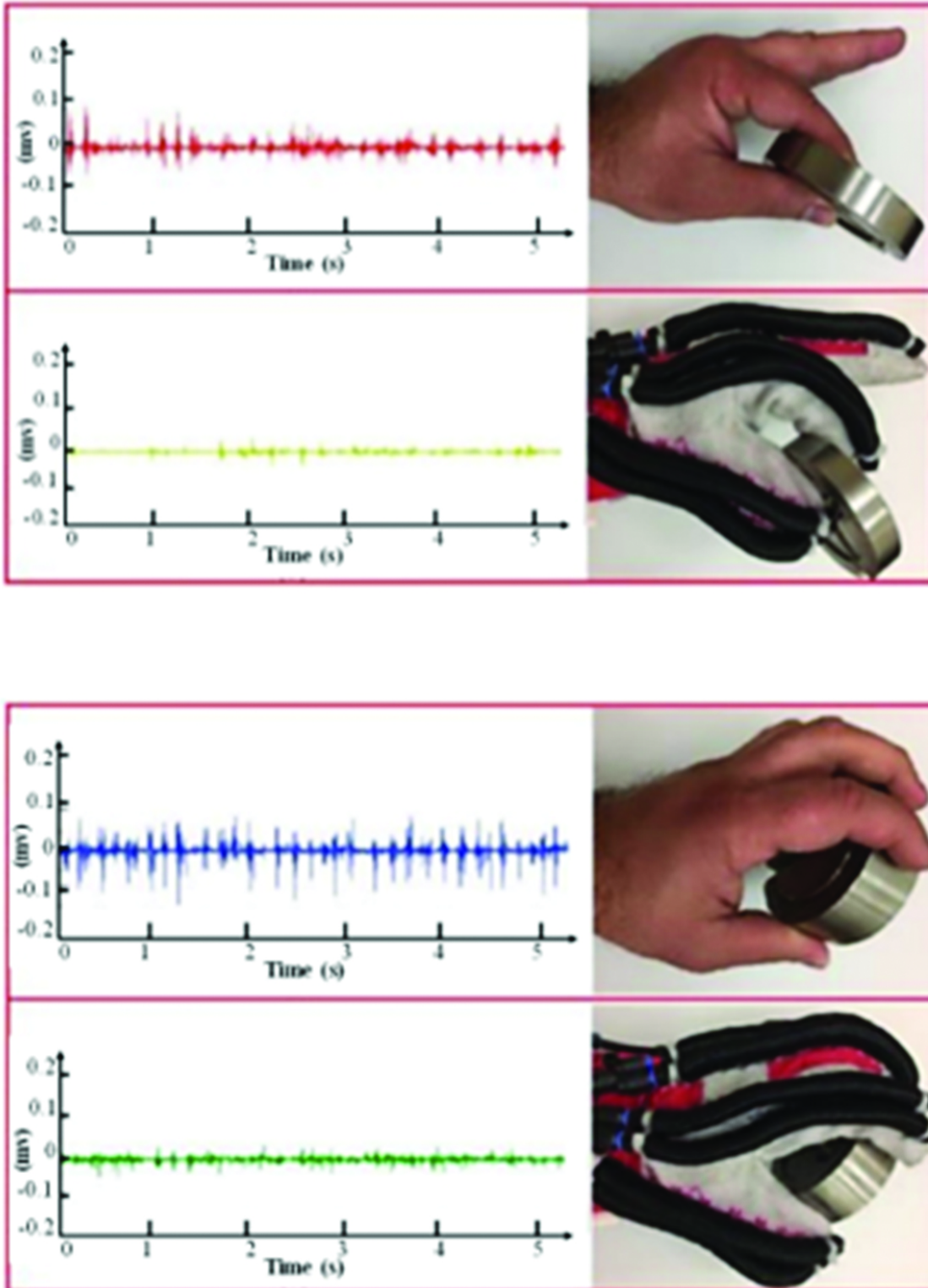
The current pressurized spacesuit design astronauts wear to perform EVAs pose challenges in ease of completing certain tasks. This is particularly the case for the hands where multiple protective layers and internal air pressure in the spacesuit limit the mobility of the hand tiring, hence much of the dexterity that the human hand possessed is lost. Soft robotics technology has the potential to assist in this area as actuators can be used to provide forces to the user's finger to augment the power to the hand muscles especially the fingers and reduce fatigue thereof.

Figure 3.31 shows a prototype force augmentation glove that uses the EBPMA. The EBPMA is used to form a hand exoskeleton to assist the bending of finger joints to perform multiple gripping and pinching movements. When pressurized, the pneumatic muscles bend and in turn apply a force to the user's fingers to amplify the power of the hand. According to [33] males and females have an average pinching force of 43 and 38 N, respectively, and experiment performed using the soft glove showed it could boost the pinching forces of a user by 40–45 percent.



*Figure 3.31 A controllable stiffness and bendable actuator and its application on soft robotic glove [32]*

To demonstrate that the force augmentation glove can reduce user fatigue, an experiment was performed using EMG (electromyography) signals taken from the user's muscles, [Figure 3.32](#). In the experiment, the test subjects were required to grasp a range of objects both with and without the glove and their muscle activity was measured using the EMG sensors. It was observed that there was a significant impact when the glove aided in grasping, and the electrical activity in the test subject's muscles reduced. This experiment did indicate the huge impact the power assistive glove allows a user to perform a task using less of their muscle force than when not using the device. Therefore, with such a glove a reduction in fatigue over time can be experienced.



*Figure 3.32 Study of the impact on human muscles when using the power assistive glove to pinch or grasp an object*

If this soft force augmentation technology were introduced into astronaut's spacesuits, it could have the potential to reduce fatigue during EVAs as the actuators would help to overcome the resistance to motion caused by the pressurized glove. The technology also has the potential to augment the astronaut's strength allowing them to perform tasks they otherwise may not be able to with their natural strength.

### **3.6 Recommendations and future works**

This chapter has introduced and discussed some of the soft robotics systems undergoing development and has looked at how this technology could potentially be used in space application in the future. While to date no soft robotic system has been used in space it is likely that this rapidly advancing field of research will see the application in space in the future. Soft robots are constructed in a very different manner and from different materials than traditional robots giving them unique behavior and abilities that conventional robots cannot provide. Thus, they are highly likely to be a viable solution for space-based challenges that cannot be addressed using existing robot technologies.

Some of the discussed advantages offered by soft robotics that make them potentially useful in space applications include:

***Low weight*** – Soft robots are typically formed from lightweight material that reduces overall system mass. In space applications, system mass is a critical factor that determines the launch and mission cost. Anything that reduces the mass of robot hardware is likely to provide financial saving. Soft robots also often have a high power-to-weight ratio meaning they can often achieve the same feats as much heavier robots do.

***Low-cost materials*** – Although little soft robotic technology is currently commercially available, most systems being developed are low cost when compared to the already established robotics technology. This factor also has the potential to reduce mission cost.

***Inherent safety*** – Soft robots are typically inherently safe due to the use of soft materials, their low weight and inertia, and their compliant actuation. This means soft robots could work collaboratively and close to an astronaut without presenting danger and also handle fragile and irregular objects. This is something much more difficult to achieve with conventional robots, especially in an unstructured environment.

***Deformable structures*** – Soft robots do not have discrete joints and they are often able to flex any part of their structure. Thus they can achieve much more complex motions than a traditional serial link manipulator can. This gives soft manipulators the ability to reach into and around obstacles and reach places a traditional robot cannot and increase the range of orbit and remote manipulation tasks that can be performed. The deformable nature of soft robots also provides advantages when grasping objects. Traditional grippers often need extensive preplanning before grasping an object, but many soft grippers can be used in an open-loop manner and will naturally deform around an object and create a secure grasp.

***Wearable*** – Soft robotics technology can easily be incorporated into lightweight, low-cost wearable devices such as exoskeleton and assistive devices. Incorporating soft actuators into an astronaut's spacesuit could enhance their abilities or reduce fatigue. Similarly, a soft body-mounted manipulator could provide an astronaut with an additional limb to help increase their productivity.

Despite the potential future advantages that soft robotic technology offers towards working and exploration in space, the technology still has several challenges that need to be overcome.

***Power sources*** – Many of the soft robotics systems developed, and indeed those described in this chapter, are pneumatic-based systems. It is the compressibility of air that gives many soft robots their desirable behavior. In a terrestrial environment, the pneumatic system is widespread with air being compressed as and when required. This is not possible in the vacuum of space and air recycling systems or another actuator technology will need to be developed.

***Sensing*** – As we have seen soft robots continuously flex and deform, and this means traditional sensors are inappropriate to monitor their motion and behavior. Advances are therefore needed in soft sensors.

***Mechanical resilience*** – To date, soft robots have seen little application outside of the laboratory environment and so they have not been designed to withstand the rigors of the environment in which they operate. Space is an extreme environment and presents a further challenge. Research and development are needed to increase the resilience of soft robots and this will require advances in materials and the development of self-repairing technology.

***Modeling and control*** – Advances are required in the modeling and control of soft robots as the already well-established techniques developed for

traditional robots are not directly applicable.

**Alternative soft technologies** – The pneumatic technology is just an example of a soft robotic system that is still under research. However, this is not the only concept of soft systems that can be used to improve and develop futuristic robots. Other technologies that are promising include SMA (Shape Memory Alloys), FEA (Fluidic Elastomeric Actuators), SMP (Shape Morphing Polymers), DEAP (Dielectric-Electrically Actuated Polymers), and E/MA (Magnetic/Electro-Magnetic Actuators).

## References

- [1] Gombolay M.C., Gutierrez R.A., Clarke S.G., Sturla G.F., Shah J.A., *et al.* ‘Decision-making authority, team efficiency and human worker satisfaction in mixed human–robot teams’. *Autonomous Robots*. 2015;**39**(3):293–312.
- [2] Di Castro M., Ferre M., Masi A. ‘CERN-TAURO: a modular architecture for robotic inspection and telemanipulation in harsh and semi-structured environments’. *IEEE Access*. 2018;**6**:37506–22.
- [3] Zanchettin A.M., Ceriani N.M., Rocco P., Ding H., Matthias B. ‘Safety in human-robot collaborative manufacturing environments: metrics and control’. *IEEE Transactions on Automation Science and Engineering*. 2016;**13**(2):882–93.
- [4] Rahman M.H., Rahman M.J., Cristobal O.L., Saad M., Kenné J.P., Archambault P.S. ‘Development of a whole arm wearable robotic exoskeleton for rehabilitation and to assist upper limb movements’. *Robotica*. 2015;**33**(1):19–39.
- [5] Reynolds E. *Nasa’s new humanoid robot to tackle space missions*. [online] Wired.co.uk. 2020. Available from [https://www.nasa.gov/mission\\_pages/station/multimedia/robonaut\\_photos.html](https://www.nasa.gov/mission_pages/station/multimedia/robonaut_photos.html) [Accessed 20 Feb 2020].
- [6] Calisti M., Giorelli M., Levy G., *et al.* ‘An octopus-bioinspired solution to movement and manipulation for soft robots’. *Bioinspiration & Biomimetics*. 2011;**6**(3):036002.
- [7] Althoff M., Giusti A., Liu S.B., Pereira A. ‘Effortless creation of safe robots from modules through self-programming and self-verification’. *Science Robotics*. 2019;**4**(31):eaaw1924.
- [8] Swaim P., Thompson C., Campbell P. ‘The Charlotte (TM) intra-vehicular robot’. *Artificial Intelligence, Robotics, and Automation for Space*

*Symposium*. 1994:157–62.

- [9] Williams R. *Automation and robotics for space-based systems-1991*. Hampton, VA: National Aeronautics and Space Administration, Langley Research Center; 1992.
- [10] Morris A., Barker L. *Technology Demonstration of Space intravehicular Automation and Robotics*; 1994.
- [11] robonaut.jsc.nasa.gov. Robonaut. [online]. n.d. Available from <https://robonaut.jsc.nasa.gov/R1/index.asp> [Accessed 9 Aug 2020].
- [12] Ahlstrom T., Curtis A., Diftler M., et al. Robonaut 2 on the International Space Station: Status update and preparations for IVA mobility. In *Aiaa Space 2013 Conference and Exposition* ; 2013. p. 5340.
- [13] General Disclaimer. [online]. n.d. Available from <https://ntrs.nasa.gov/archive/nasa/casi.ntrs.nasa.gov/19760003644.pdf> [Accessed 3 Aug 2020].
- [14] Waldie J.M.A.T. ‘Compression under a mechanical counter pressure space suit glove’. *Journal of Gravitational Physiology: A Journal of the International Society for Gravitational Physiology [online]*. 2002:93–7.
- [15] Tanaka K., Danaher P., Webb P., Hargens A.R. ‘Mobility of the elastic counterpressure space suit glove’. *Aviation, Space, and Environmental Medicine*. 2009;**80**(10):890–3.
- [16] Sanner R., Sorenson B., Fogleman M., Hq N., Kosmo M., Jsc N. NASA research announcement phase h final report for the development of a power assisted space suit glove [online]. 1997. Available from <https://ntrs.nasa.gov/archive/nasa/casi.ntrs.nasa.gov/19980007975.pdf> [Accessed 3 Aug 2020].
- [17] Konkel C.R., Powers A.K., Dewitt J.R. IVA the robot: Design guidelines and lessons learned from the first space station laboratory manipulation system. In *Fourth Annual Workshop on Space Operations Applications and Research (SOAR'90): Proceedings of a Workshop Sponsored by the National Aeronautics and Space Administration*, Vol. 1; Washington, DC, the US Air Force, Washington, DC, and Cosponsored by the University of New Mexico, Albuquerque, New Mexico, and Held in Albuquerque, New Mexico, June 26-28, 1990, National Aeronautics and Space Administration; 1991, January. p. 9.
- [18] Fantoni G., Santochi M., Dini G., et al. ‘Grasping devices and methods in automated production processes’. *CIRP Annals*. 2014;**63**(2):679–701.

- [19] Choi H., Koç M. ‘Design and feasibility tests of a flexible gripper based on inflatable rubber pockets’. *International Journal of Machine Tools and Manufacture*. 2006;**46**(12):1350–61.
- [20] Caldwell D.G., Tsagarakis N., Medrano-Cerda G.A., Schofield J., Brown S. ‘A pneumatic muscle actuator driven manipulator for nuclear waste retrieval’. *Control Engineering Practice*. 2001;**9**(1):23–36.
- [21] Martell J., Gini G. ‘Robotic hands: design review and proposal of new design process’. *Image*. 2007;**180**:9270.
- [22] Jamwal P.K., Xie S.Q. ‘Artificial neural network based dynamic modelling of indigenous pneumatic muscle actuators’. Paper presented at the 2012 IEEE/ASME International Conference on Mechatronics and Embedded Systems and Applications (MESA); 2012.
- [23] Andrikopoulos G., Nikolakopoulos G., Manesis S. ‘Advanced nonlinear PID-based antagonistic control for pneumatic muscle actuators’. *IEEE Transactions on Industrial Electronics*. 2014;**61**(12):6926–37.
- [24] Tondu B. ‘Modelling of the McKibben artificial muscle: a review’. *Journal of Intelligent Material Systems and Structures*. 2012;**23**(3):225–53.
- [25] Trivedi D., Rahn C.D., Kier W.M., Walker I.D. ‘Soft robotics: biological inspiration, state of the art, and future research’. *Applied Bionics and Biomechanics*. 2008;**5**(3):99–117.
- [26] Tatlicioglu E., Walker I.D., Dawson D.M. ‘Dynamic modelling for planar extensible continuum robot manipulators’. Paper presented at the 2007 IEEE International Conference on Robotics and Automation; 2007.
- [27] Kelasidi E., Andrikopoulos G., Nikolakopoulos G., Manesis S. ‘A survey on pneumatic muscle actuators modeling’. Paper presented at the 2011 IEEE International Symposium on Industrial Electronics (ISIE); 2011.
- [28] Ching-PingChou., Hannaford B. ‘Measurement and modeling of McKibben pneumatic artificial muscles’. *IEEE Transactions on Robotics and Automation*. 1996;**12**(1):90–102.
- [29] Tondu B., Lopez P. ‘Modeling and control of McKibben artificial muscle robot actuators’. *Control Systems, IEEE*. 2000;**20**(2):15–38.
- [30] Al-Ibadi A., Nefti-Meziani S., Davis S. ‘Controlling of pneumatic muscle actuator systems by parallel structure of neural network and proportional controllers (PNNP)’. *Frontiers in Robotics and AI, section Soft Robotics*. 2020;7.
- [31] Al-Ibadi A., Nefti-Meziani S., Davis S. ‘The design, kinematics and torque analysis of the self-bending soft contraction actuator’. *Actuators*.

2020;**9**(2):33.

- [32] Al-Ibadi A., Nefti-Meziani S., Davis S., Theodoridis T. ‘Novel design and position control strategy of a soft robot arm’. *Robotics*. 2018;**7**(4):72.
- [33] Kadowaki Y., Noritsugu T., Takaiwa M., Sasaki D., Kato M ‘Development of soft power-assist glove and control based on human intent’. *Journal of Robotics and Mechatronics*. 2011;**23**(2):281–91.

[30] Al-Ibadi, A., Nefti-Meziani, S. and Davis, S., 2020. Controlling of pneumatic muscle actuator systems by Parallel Structure of Neural Network and Proportional Controllers (PNNP). *Frontiers in Robotics and AI*, 7, p.115.

[31] Al-Ibadi, A., Nefti-Meziani, S. and Davis, S., 2020, June. The design, kinematics and torque analysis of the self-bending soft contraction actuator. In *Actuators* (Vol. 9, No. 2, p. 33). Multidisciplinary Digital Publishing Institute.